# Computational Materials Physics

## Density Functional Theory

**Physics Concerto**

**2023 November 8th**

$$\left(-\sum_i \frac{\nabla_i^2}{2} - \sum_I \frac{\nabla_I^2}{2M_I} - \sum_{i,I}\frac{Z_I}{|\mathbf{r}_i-\mathbf{R}_I|} + \frac{1}{2}\sum_{i\neq j}\frac{1}{|\mathbf{r}_i-\mathbf{r}_j|} + \frac{1}{2}\sum_{I\neq J}\frac{Z_I Z_J}{|\mathbf{R}_I-\mathbf{R}_J|}\right)\Psi = E_{\mathrm{tot}}\Psi.$$

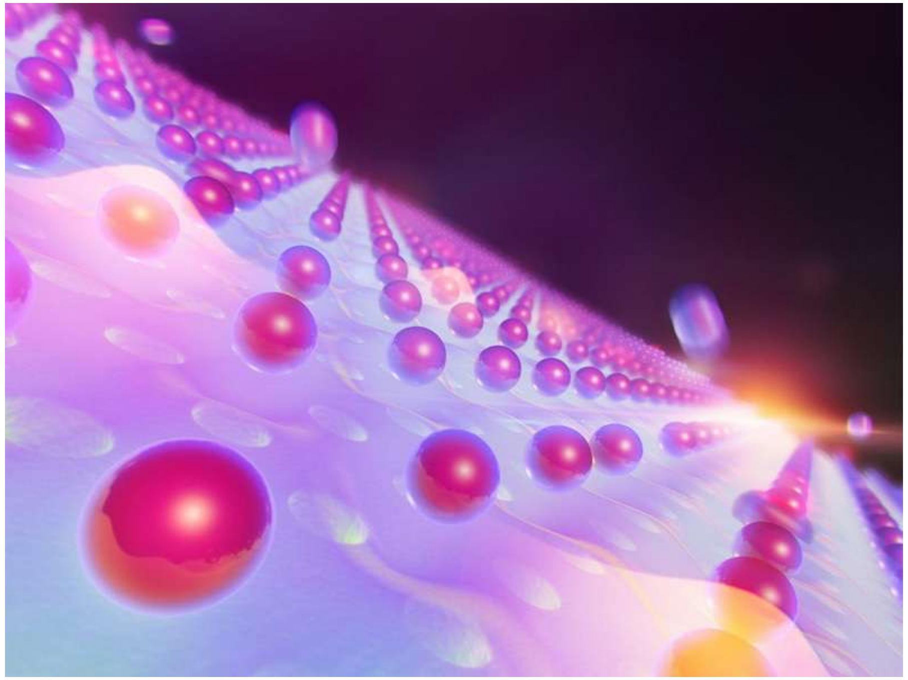

## James R Chelikowsky

Professor, Core Faculty, Oden Institute
W. A. "Tex" Moncrief, Jr. Chair in Computational Materials (Holder)

*Computational materials science; solid state physics.*

512-232-9083
POB 4.324
Email »
Full Profile »

## Alexander A Demkov

Professor, Affiliated Faculty, Oden Institute
*Condensed matter theory; physics of electronic materials; surfaces, interfaces, thin films and devices; novel materials, quantum transport*

512-471-1153
PMA 13.206
Email »
Full Profile »

## Feliciano Giustino

Professor, Core Faculty, Oden Institute
W.A. "Tex" Moncrief, Jr. Endowment in Simulation-Based Engineering and Sciences - Endowed Chair No. 6 (Holder)

*Condensed Matter Theory, Computational*

512-232-5755
POB
Email »
Full Profile »

## Allan H Macdonald

Professor
Sid W. Richardson Foundation Regents Chair in Physics #1 (Holder)

*Condensed matter theory*

512-232-7960
PMA
Email »
Full Profile »

10 more professors in Chemistry, ECE, ME, Materials E, …

# Computational Materials Physics

$$\left(-\sum_i \frac{\nabla_i^2}{2} - \sum_I \frac{\nabla_I^2}{2M_I} - \sum_{i,I} \frac{Z_I}{|\mathbf{r}_i - \mathbf{R}_I|} + \frac{1}{2}\sum_{i\neq j} \frac{1}{|\mathbf{r}_i - \mathbf{r}_j|} + \frac{1}{2}\sum_{I\neq J} \frac{Z_I Z_J}{|\mathbf{R}_I - \mathbf{R}_J|}\right)\Psi = E_{\text{tot}}\Psi.$$

Thousands of Physicists
Billions of dollars
Bad for environment

Courtesy of the National Pest Management Association / Tom Myers

What would you do first?


Some chemists
$5
Eco-friendly

# Density Functional Theory

## Generalized gradient approximation made simple

### Authors

John P Perdew, Kieron Burke, Matthias Ernzerhof

### Publication date

1996/10/28

### Journal

Physical review letters

### Total citations

Cited by 173259

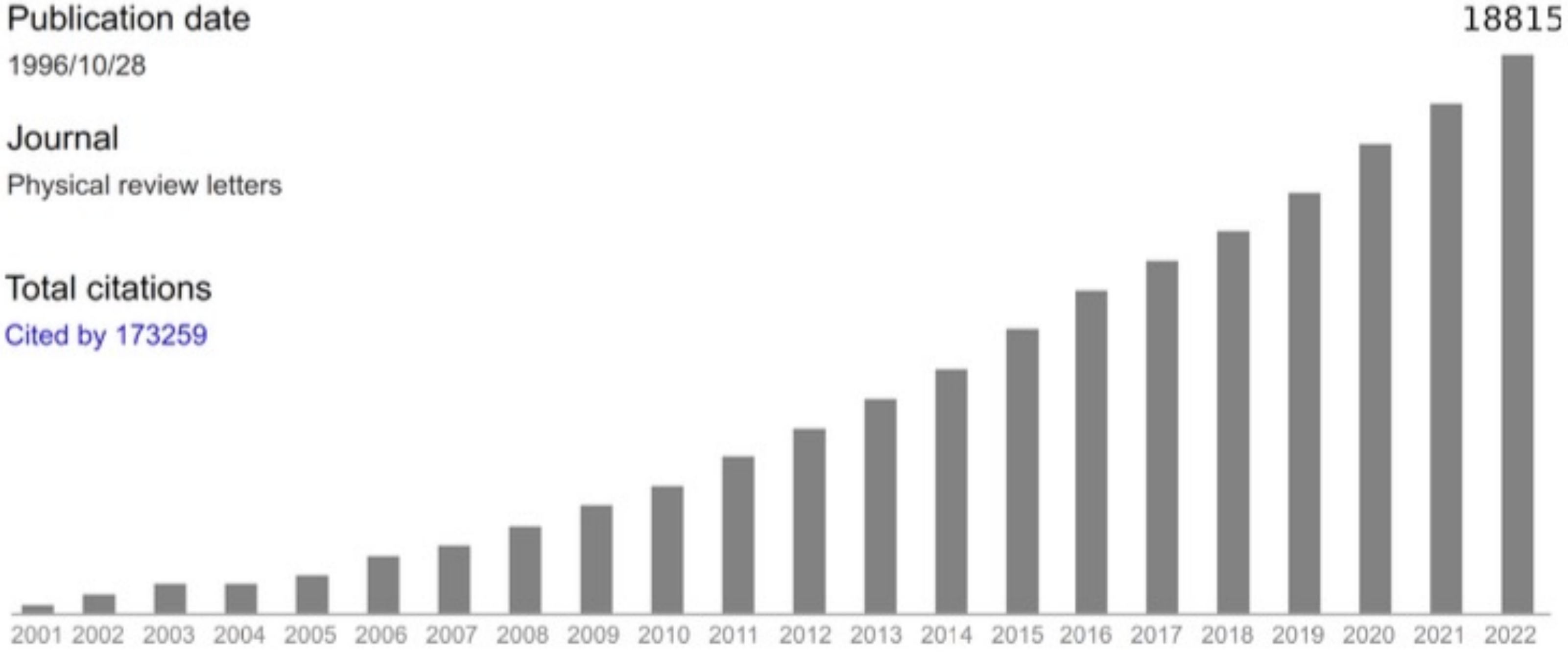

# Density Functional Theory

**1964** Hohenberg–Kohn theorem and Kohn–Sham formulation

**1972** Relativistic extension of density functional theory

**1980** Local density approximation for exchange and correlation

**1984** Time-dependent density functional theory

**1985** First-principles molecular dynamics

**1986** Quasiparticle corrections for insulators

**1987** Density functional perturbation theory

**1988** Towards quantum chemistry accuracy

**1991** Hubbard-corrected density functional theory

**1996** The generalized gradient approximation

# Density Functional Theory

You've never heard spin today… but works perfectly for a magnetic system as well.

$$\left(-\sum_i \frac{\nabla_i^2}{2} - \cancel{\sum_I \frac{\nabla_I^2}{2M_I}} - \sum_{i,I} \frac{Z_I}{|\mathbf{r}_i - \mathbf{R}_I|} + \frac{1}{2}\sum_{i\neq j} \frac{1}{|\mathbf{r}_i - \mathbf{r}_j|} + \frac{1}{2}\sum_{I\neq J} \frac{Z_I Z_J}{|\mathbf{R}_I - \mathbf{R}_J|}\right)\Psi = E_{\text{tot}}\Psi.$$

Clamped nuclei

$$\Bigg(\underbrace{-\sum_i \frac{\nabla_i^2}{2} - \sum_{i,I} \frac{Z_I}{|\mathbf{r}_i - \mathbf{R}_I|}}_{\text{single-electron}} + \underbrace{\frac{1}{2}\sum_{i\neq j} \frac{1}{|\mathbf{r}_i - \mathbf{r}_j|}}_{\text{many-electron}}\Bigg)\Psi = E\,\Psi. \qquad E = E_{\text{tot}} - \frac{1}{2}\sum_{I\neq J} \frac{Z_I Z_J}{|\mathbf{R}_I - \mathbf{R}_J|}.$$

$$\hat{H}(\mathbf{r}_1, \ldots, \mathbf{r}_N) = \sum_i \hat{H}_0(\mathbf{r}_i) + \frac{1}{2}\sum_{i\neq j} \frac{1}{|\mathbf{r}_i - \mathbf{r}_j|}$$

$$n(\mathbf{r}) = \sum_i |\phi_i(\mathbf{r})|^2$$

$$\Psi(\mathbf{r}_1, \mathbf{r}_2, \cdots, \mathbf{r}_N) = \phi_1(\mathbf{r}_1)\cdots\phi_N(\mathbf{r}_N)$$

Independent electron approximation

$$\Psi(\mathbf{r}_1, \mathbf{r}_2) = \frac{1}{\sqrt{2}}\begin{vmatrix} \phi_1(\mathbf{r}_1) & \phi_1(\mathbf{r}_2) \\ \phi_2(\mathbf{r}_1) & \phi_2(\mathbf{r}_2) \end{vmatrix}$$

Slater determinant

# Density Functional Theory

$$\Bigg(\underbrace{-\sum_i \frac{\nabla_i^2}{2} - \sum_{i,I} \frac{Z_I}{|\mathbf{r}_i - \mathbf{R}_I|}}_{\text{single-electron}} + \underbrace{\frac{1}{2}\sum_{i\neq j} \frac{1}{|\mathbf{r}_i - \mathbf{r}_j|}}_{\text{many-electron}}\Bigg)\Psi = E\,\Psi. \qquad \Psi(\mathbf{r}_1, \mathbf{r}_2, \cdots, \mathbf{r}_N) = \phi_1(\mathbf{r}_1)\cdots\phi_N(\mathbf{r}_N)$$

$$\left[-\frac{\nabla^2}{2} + V_{\mathrm{n}}(\mathbf{r}) + V_{\mathrm{H}}(\mathbf{r})\right]\phi_i(\mathbf{r}) = \varepsilon_i\,\phi_i(\mathbf{r})$$

Hartree or mean-field approximation

$$n(\mathbf{r}) = \sum_i |\phi_i(\mathbf{r})|^2,$$

$$\nabla^2 V_{\mathrm{H}}(\mathbf{r}) = -4\pi n(\mathbf{r}).$$

Self-consistent field method

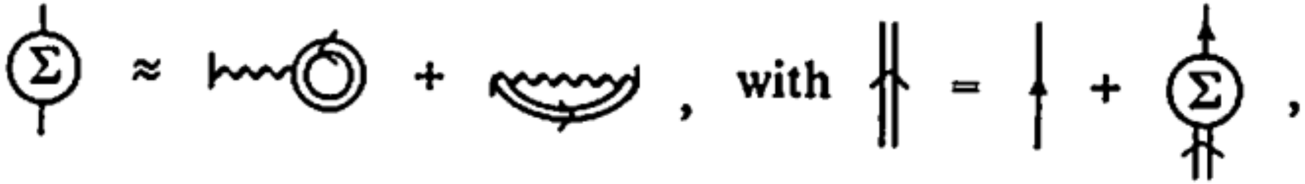

# Density Functional Theory

$$\Bigg(\underbrace{-\sum_i \frac{\nabla_i^2}{2} - \sum_{i,I} \frac{Z_I}{|\mathbf{r}_i - \mathbf{R}_I|}}_{\text{single-electron}} + \underbrace{\frac{1}{2}\sum_{i\neq j} \frac{1}{|\mathbf{r}_i - \mathbf{r}_j|}}_{\text{many-electron}}\Bigg)\Psi = E\,\Psi. \qquad \Psi(\mathbf{r}_1, \mathbf{r}_2, \cdots, \mathbf{r}_N) = \phi_1(\mathbf{r}_1)\cdots\phi_N(\mathbf{r}_N)$$

$$\left[-\frac{\nabla^2}{2} + V_{\mathrm{n}}(\mathbf{r}) + V_{\mathrm{H}}(\mathbf{r})\right]\phi_i(\mathbf{r}) + \underbrace{\int d\mathbf{r}'\, V_{\mathrm{X}}(\mathbf{r}, \mathbf{r}')\,\phi_i(\mathbf{r}')}_{\text{Including exchange interaction}} = \varepsilon_i\,\phi_i(\mathbf{r}),$$

$$n(\mathbf{r}) = \sum_i |\phi_i(\mathbf{r})|^2,$$

$$\nabla^2 V_{\mathrm{H}}(\mathbf{r}) = -4\pi n(\mathbf{r}).$$

$$V_{\mathrm{H}}(\mathbf{r}) = \sum_j \int d\mathbf{r}' \frac{|\phi_j(\mathbf{r}')|^2}{|\mathbf{r} - \mathbf{r}'|}, \qquad V_{\mathrm{X}}(\mathbf{r}, \mathbf{r}') = -\sum_j \frac{\phi_j^*(\mathbf{r}')\phi_j(\mathbf{r})}{|\mathbf{r} - \mathbf{r}'|}.$$

Self-interaction for localized orbitals

Nonlocal

# Density Functional Theory


Nobel prize in Chemistry 1998

Schwinger's student

$E$ is the energy of the ground state: $n(\mathbf{r}) \xrightarrow{F} E \quad E = F[n(\mathbf{r})]$

$E$ is the energy of an excited state: $\Psi(\mathbf{r}_1, \ldots, \mathbf{r}_N) \xrightarrow{\mathcal{F}} E \quad E = \mathcal{F}[\Psi(\mathbf{r}_1, \ldots, \mathbf{r}_N)]$

Hohenberg-Kohn theorem

$$\left.\frac{\delta F[n]}{\delta n}\right|_{n_0} = 0.$$

$$E = \langle \Psi | \hat{H} | \Psi \rangle = \int d\mathbf{r}_1 \ldots d\mathbf{r}_N \, \Psi^*(\mathbf{r}_1, \ldots, \mathbf{r}_N) \, \hat{H} \, \Psi(\mathbf{r}_1, \ldots, \mathbf{r}_N). \tag{3.1}$$

$$\hat{H}(\mathbf{r}_1, \mathbf{r}_2, \cdots, \mathbf{r}_N) = -\sum_i \frac{1}{2}\nabla_i^2 + \sum_i V_{\text{n}}(\mathbf{r}_i) + \frac{1}{2}\sum_{i \neq j} \frac{1}{|\mathbf{r}_i - \mathbf{r}_j|}. \tag{3.2}$$

1) In the ground state the electron density determines uniquely the external potential $V_{\text{n}}$ in eqn 3.2: $n \to V_{\text{n}}$.
2) In any quantum state the external potential, $V_{\text{n}}$, determines uniquely the many-electron wavefunction: $V_{\text{n}} \to \Psi$.
3) In any quantum state the total energy, $E$, is a functional of the many-body wavefunction through eqn 3.1: $\Psi \to E$.

The ground state energy of a many-electron system is expressed as a functional of the electron density!

Density Functional Theory!

# Density Functional Theory

$E$ is the energy of the ground state: $n(\mathbf{r}) \xrightarrow{F} E \quad E = F[n(\mathbf{r})]$

Hohenberg-Kohn theorem $\left.\frac{\delta F[n]}{\delta n}\right|_{n_0} = 0.$

$$\boxed{\left(-\sum_i \frac{\nabla_i^2}{2} - \sum_I \frac{\nabla_I^2}{2M_I} - \sum_{i,I} \frac{Z_I}{|\mathbf{r}_i - \mathbf{R}_I|} + \frac{1}{2}\sum_{i\neq j} \frac{1}{|\mathbf{r}_i - \mathbf{r}_j|} + \frac{1}{2}\sum_{I\neq J} \frac{Z_I Z_J}{|\mathbf{R}_I - \mathbf{R}_J|}\right)\Psi = E_{\text{tot}}\Psi.}$$

$$F[n] = \int d\mathbf{r}\, n(\mathbf{r}) V_{\text{n}}(\mathbf{r}) - \sum_i \int d\mathbf{r}\, \psi_i^*(\mathbf{r}) \frac{\nabla^2}{2} \psi_i(\mathbf{r}) + \frac{1}{2} \iint d\mathbf{r} d\mathbf{r}' \frac{n(\mathbf{r}) n(\mathbf{r}')}{|\mathbf{r} - \mathbf{r}'|} + E_{xc}[n].$$

$$\boxed{\left[-\frac{1}{2}\nabla^2 + V_{\text{n}}(\mathbf{r}) + V_{\text{H}}(\mathbf{r}) + V_{xc}(\mathbf{r})\right]\phi_i(\mathbf{r}) = \varepsilon_i \phi_i(\mathbf{r}).}$$

Kohn-Sham equation

Walter Kohn

Kohn in 2012

Nothing but just Hartree potential…

*'The Kohn-Sham theory may be regarded as the formal exactification of Hartree theory. With the exact $E_{xc}$ and $V_{xc}$ all many-body effects are in principle included. Clearly this directs attention to the functional $E_{xc}[n]$. The practical usefulness of ground-state DFT depends entirely on whether approximations for the functional $E_{xc}[n]$ could be found, which are at the same time sufficiently simple and sufficiently accurate.'*

# Density Functional Theory

But how can we determine exchange-correlation potential?

Assume homogeneous electron gas first

$$E_{\mathrm{X}} = -\frac{3}{4}\left(\frac{3}{\pi}\right)^{\frac{1}{3}} n^{\frac{4}{3}} V.$$

$$E_{\mathrm{C}} = nV \cdot \begin{cases} 0.0311\ln r_s - 0.0480 + 0.002\, r_s \ln r_s - 0.0116\, r_s & \text{if } r_s < 1, \\ \dfrac{-0.1423}{1 + 1.0529\sqrt{r_s} + 0.3334\, r_s} & \text{if } r_s \geq 1. \end{cases}$$

From stochastic Monte Carlo

$$E_{\text{correl. (high density)}} = 0{\cdot}046 + A^{(2)} \int \frac{d^3\mathbf{q}}{q^3} + r_s A^{(3)} \int \frac{d^3\mathbf{q}}{q^5} + r_s^2 A^{(4)} \int \frac{d^3\mathbf{q}}{q^7} + \cdots$$

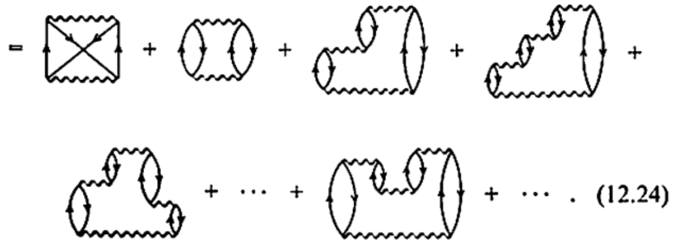


$$\frac{E_{\text{correl.}}}{N} = 0{\cdot}0622 \ln r_s - 0{\cdot}096 + \mathcal{O}(r_s),$$

First two terms are by Gell-Mann and Brueckner (1957)

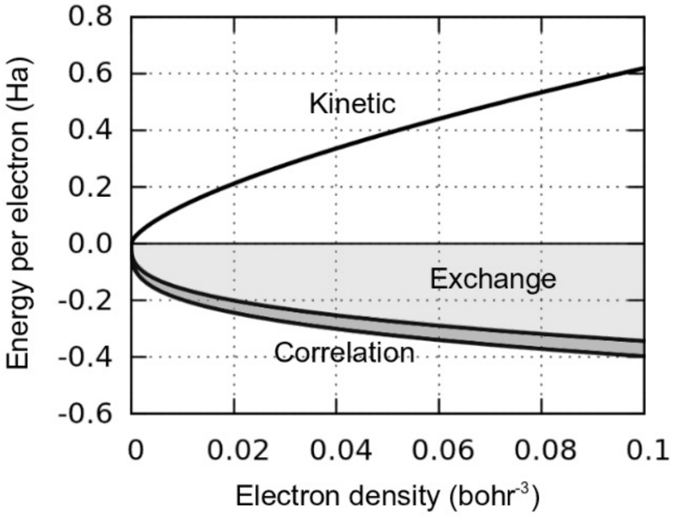


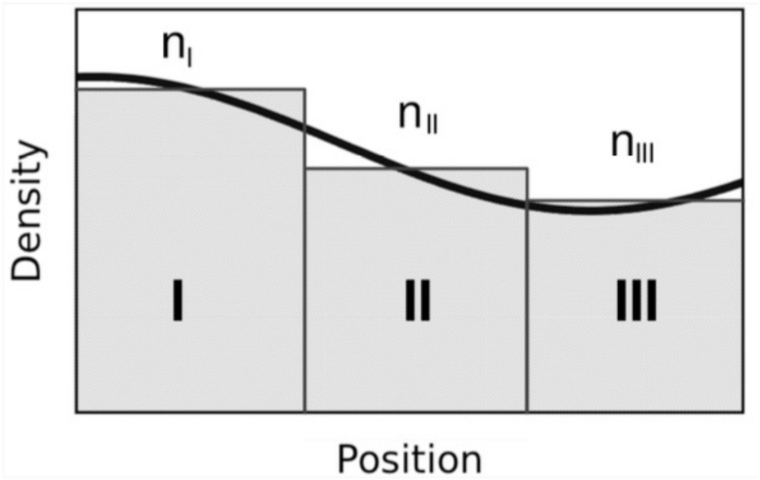




Feliciano Giustino, Materials Modeling using Density Functional Theory (2014)
Richard D. Mattuck, A Guide to Feynman Diagrams in the Many-Body Problem (1992)

# Density Functional Theory

$$\left[-\frac{1}{2}\nabla^2 + V_{\mathrm{tot}}(\mathbf{r})\right]\phi_i(\mathbf{r}) = \varepsilon_i\phi_i(\mathbf{r}),$$

$$V_{\mathrm{tot}}(\mathbf{r}) = V_{\mathrm{n}}(\mathbf{r}) + V_{\mathrm{H}}(\mathbf{r}) + V_{xc}(\mathbf{r}),$$

$$V_{\mathrm{n}}(\mathbf{r}) = -\sum\nolimits_I \frac{Z_I}{|\mathbf{r}-\mathbf{R}_I|},$$

$$\nabla^2 V_{\mathrm{H}}(\mathbf{r}) = -4\pi n(\mathbf{r}),$$

$$V_{xc}(\mathbf{r}) = \frac{\delta E_{xc}[n]}{\delta n}(\mathbf{r}),$$

$$n(\mathbf{r}) = \sum\nolimits_i |\phi_i(\mathbf{r})|^2.$$

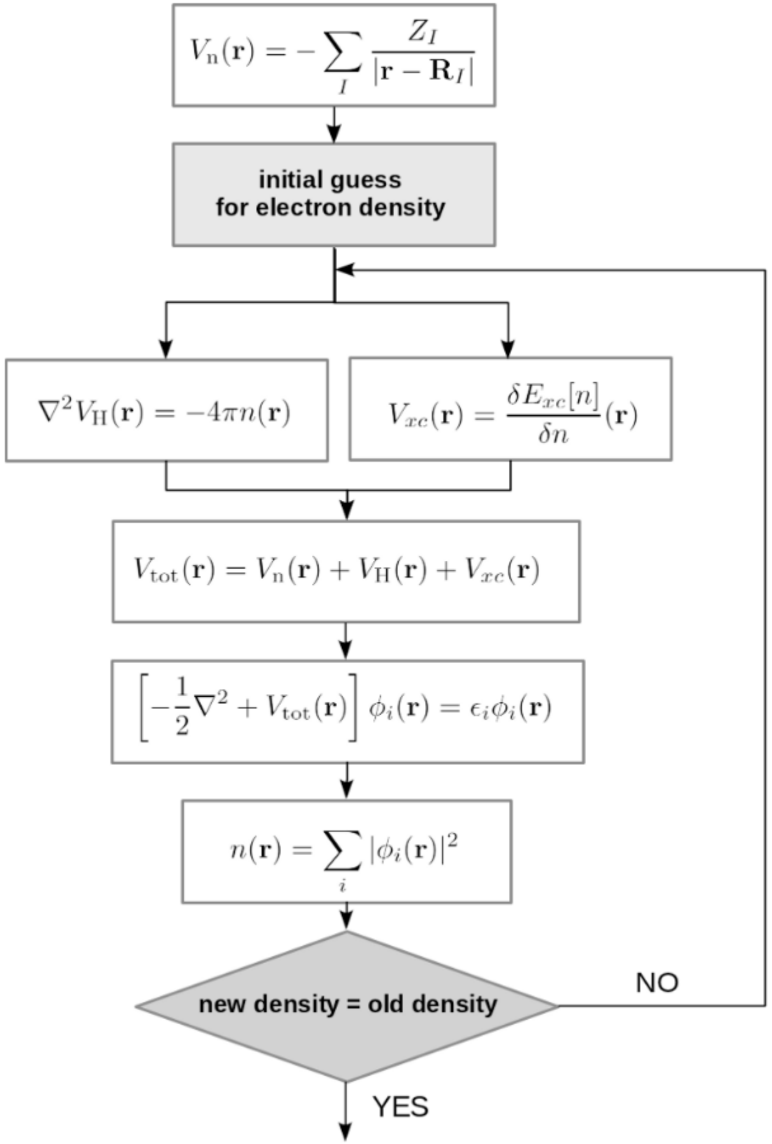


Self-consistent calculation!

Energy, charge density

# Planewaves Representation

$$\boxed{\left[-\frac{1}{2}\nabla^2 + V_{\mathrm{n}}(\mathbf{r}) + V_{\mathrm{H}}(\mathbf{r}) + V_{xc}(\mathbf{r})\right]\phi_i(\mathbf{r}) = \varepsilon_i\phi_i(\mathbf{r}).}$$

$$6\Phi(p,q,r) - [\Phi(p+1,q,r) + \Phi(p-1,q,r) + \Phi(p,q+1,r) + \Phi(p,q-1,r)$$
$$+\Phi(p,q,r+1) + \Phi(p,q,r-1)] + 2\left(\frac{a}{N_p}\right)^2 V_{\mathrm{tot}}(p,q,r)\Phi(p,q,r) = 2\left(\frac{a}{N_p}\right)^2 \varepsilon\,\Phi(p,q,r).$$

$$H\begin{bmatrix}\Phi(1)\\ \Phi(2)\\ \dots\\ \Phi(N_p^3)\end{bmatrix} = \varepsilon\begin{bmatrix}\Phi(1)\\ \Phi(2)\\ \dots\\ \Phi(N_p^3)\end{bmatrix},$$

$N_p$ ~ 200

real space representation requires too many data points to solve the differential equation

$$\mathbf{G} = m_1\mathbf{b}_1 + m_2\mathbf{b}_2 + m_3\mathbf{b}_3,\ \text{with } m_1, m_2, m_3 \text{ integers.}$$

$$\phi(\mathbf{r}) = \sum\nolimits_{\mathbf{G}} c(\mathbf{G})\exp(i\mathbf{G}\cdot\mathbf{r}).$$

$$c(\mathbf{G}) = \frac{1}{a^3}\int d\mathbf{r}\exp(-i\mathbf{G}\cdot\mathbf{r})\phi(\mathbf{r})\,.$$

$$\exp[i\mathbf{G}\cdot(\mathbf{r}+a\mathbf{u}_x)] = \exp(i\mathbf{G}\cdot\mathbf{r})\exp(ia\mathbf{G}\cdot\mathbf{u}_x) = \exp(i\mathbf{G}\cdot\mathbf{r})\exp(i2\pi m_1) = \exp(i\mathbf{G}\cdot\mathbf{r}),$$

Periodicity is implemented automatically

$$\frac{|\mathbf{G}|^2}{2}c(\mathbf{G}) + \sum\nolimits_{\mathbf{G}'} v_{\mathrm{tot}}(\mathbf{G}-\mathbf{G}')c(\mathbf{G}') = \varepsilon\, c(\mathbf{G}),$$

Expensive part

# Pseudopotential

$$\left[-\frac{1}{2}\nabla^2 + V_{\mathrm{n}}(\mathbf{r}) + V_{\mathrm{H}}(\mathbf{r}) + V_{xc}(\mathbf{r})\right] \phi_i(\mathbf{r}) = \varepsilon_i \phi_i(\mathbf{r}).$$

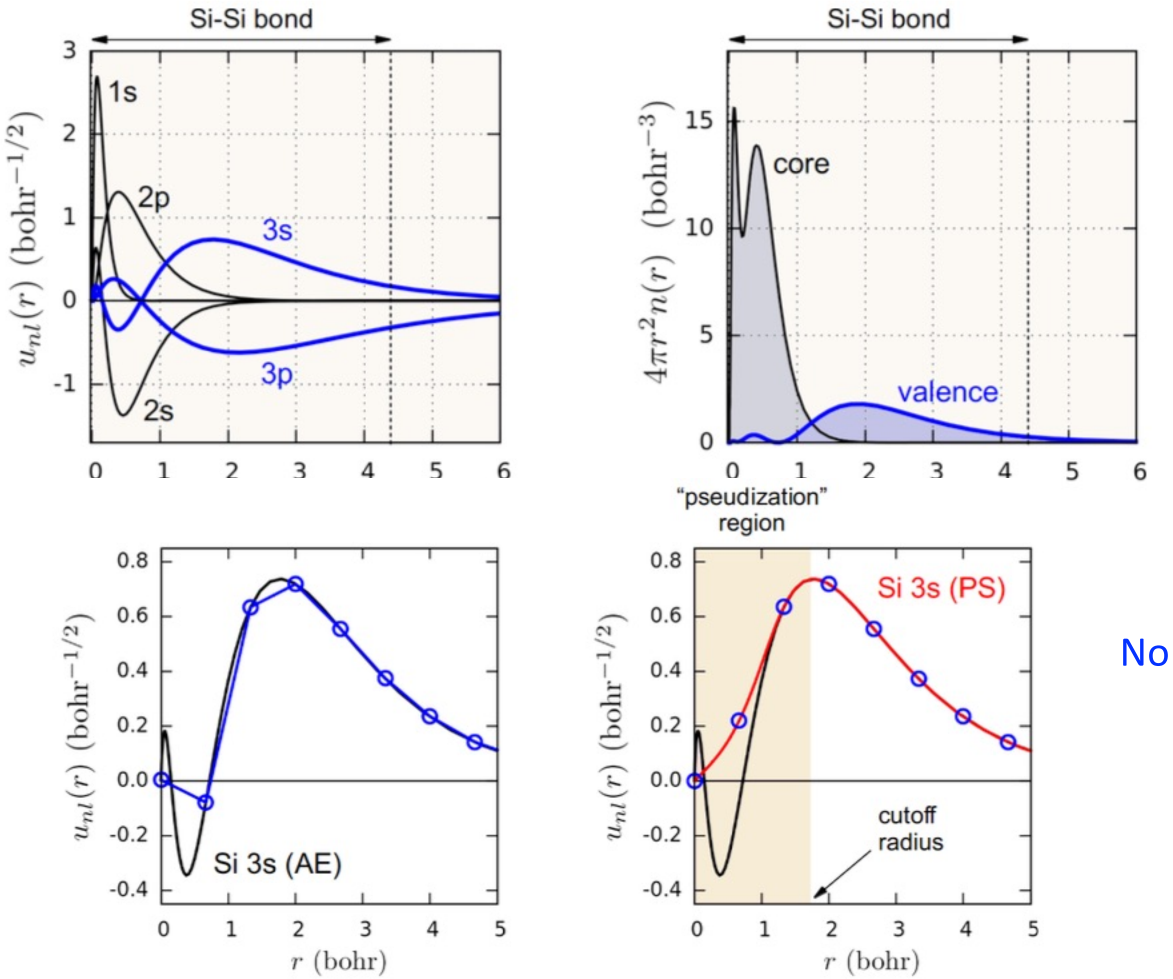


Norm-conserved Pseudopotential
Ultrasoft Pseudopotential
Projector Augmented Wave

# Total Energy and Eigenfunctions

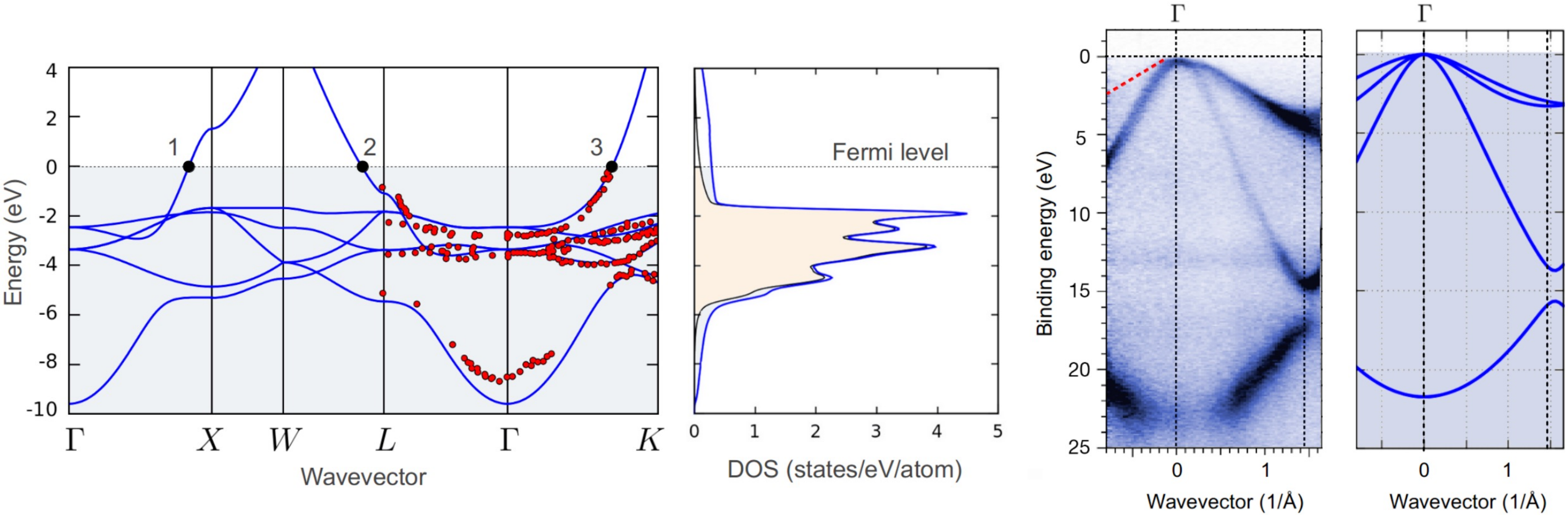

# Taylor Expansion of the Total Energy

What are we going to do with the energy?

$$E(u, \mathcal{E}, \eta) = E_0 +$$



Wu, Vanderbilt, and Hamann, Systematic treatment of displacements, strains, and electric fields in density-functional perturbation theory, Physical Review B **72**, 035105 (2005)

# Taylor Expansion of the Total Energy

$$E(u, \mathcal{E}, \eta) = E_0 +$$

$$\frac{\partial E}{\partial u_m} u_m + \frac{\partial E}{\partial \mathcal{E}_\alpha} \mathcal{E}_\alpha + \frac{\partial E}{\partial \eta_j} \eta_j +$$

Forces | Polarization | Stress

$$\frac{1}{2} \frac{\partial^2 E}{\partial u_m \partial u_n} u_m u_n + \frac{1}{2} \frac{\partial^2 E}{\partial \mathcal{E}_\alpha \partial \mathcal{E}_\beta} \mathcal{E}_\alpha \mathcal{E}_\beta + \frac{1}{2} \frac{\partial^2 E}{\partial \eta_i \partial \eta_j} \eta_i \eta_j + \frac{1}{2} \frac{\partial^2 E}{\partial u_m \partial \mathcal{E}_\alpha} u_m \mathcal{E}_\alpha + \frac{1}{2} \frac{\partial^2 E}{\partial u_m \partial \eta_j} u_m \eta_j + \frac{1}{2} \frac{\partial^2 E}{\partial \mathcal{E}_\alpha \partial \eta_j} \mathcal{E}_\alpha \eta_j +$$

Harmonic force constants | Dielectric susceptibility | Elastic moduli | Born-effective charges | Force response of the internal strain tensor | Piezoelectric strain tensor

$$\frac{1}{6} \frac{\partial^3 E}{\partial \mathcal{E}_\alpha \partial \mathcal{E}_\beta \partial \mathcal{E}_\gamma} \mathcal{E}_\alpha \mathcal{E}_\beta \mathcal{E}_\gamma + \frac{1}{6} \frac{\partial^3 E}{\partial \mathcal{E}_\alpha \partial \mathcal{E}_\beta \partial u_m} \mathcal{E}_\alpha \mathcal{E}_\beta u_m + \frac{1}{6} \frac{\partial^3 E}{\partial \mathcal{E}_\alpha \partial \mathcal{E}_\beta \partial \eta_i} \mathcal{E}_\alpha \mathcal{E}_\beta \eta_i + \cdots$$

Nonlinear susceptibility | Raman susceptibility matrix elements | Elasto-optic tensor


Wu, Vanderbilt, and Hamann, Systematic treatment of displacements, strains, and electric fields in density-functional perturbation theory, Physical Review B **72**, 035105 (2005)

# Taylor Expansion of the Total Energy

$$E(u,\mathcal{E},\eta) = E_0 +$$

$$\frac{\partial E}{\partial u_m}u_m + \frac{\partial E}{\partial \mathcal{E}_\alpha}\mathcal{E}_\alpha + \frac{\partial E}{\partial \eta_j}\eta_j +$$

Hellmann-Feynman

Modern Theory of Polarization

Stress Theorem

$$\frac{1}{2}\frac{\partial^2 E}{\partial u_m \partial u_n}u_m u_n + \frac{1}{2}\frac{\partial^2 E}{\partial \mathcal{E}_\alpha \partial \mathcal{E}_\beta}\mathcal{E}_\alpha\mathcal{E}_\beta + \frac{1}{2}\frac{\partial^2 E}{\partial \eta_i \partial \eta_j}\eta_i\eta_j + \frac{1}{2}\frac{\partial^2 E}{\partial u_m \partial \mathcal{E}_\alpha}u_m\mathcal{E}_\alpha + \frac{1}{2}\frac{\partial^2 E}{\partial u_m \partial \eta_j}u_m\eta_j + \frac{1}{2}\frac{\partial^2 E}{\partial \mathcal{E}_\alpha \partial \eta_j}\mathcal{E}_\alpha\eta_j +$$

DFPT

DFPT
Finite electric field

DFPT

DFPT
Finite electric field

DFPT

DFPT
Finite electric field

$$\frac{1}{6}\frac{\partial^3 E}{\partial \mathcal{E}_\alpha \partial \mathcal{E}_\beta \partial \mathcal{E}_\gamma}\mathcal{E}_\alpha\mathcal{E}_\beta\mathcal{E}_\gamma + \frac{1}{6}\frac{\partial^3 E}{\partial \mathcal{E}_\alpha \partial \mathcal{E}_\beta \partial u_m}\mathcal{E}_\alpha\mathcal{E}_\beta u_m + \frac{1}{6}\frac{\partial^3 E}{\partial \mathcal{E}_\alpha \partial \mathcal{E}_\beta \partial \eta_i}\mathcal{E}_\alpha\mathcal{E}_\beta\eta_i + \cdots$$

2*n*+1 theorem
Finite electric field

2*n*+1 theorem
Finite electric field

2*n*+1 theorem
Finite electric field

Finite difference method

$$p_{ij\mu\nu} \approx \frac{\Delta(\varepsilon_{ij}^{-1})(\eta^+) - \Delta(\varepsilon_{ij}^{-1})(\eta^-)}{2\eta_{\mu\nu}} + \mathcal{O}(\eta^2).$$


Wu, Vanderbilt, and Hamann, Systematic treatment of displacements, strains, and electric fields in density-functional perturbation theory, Physical Review B **72**, 035105 (2005)

The University of Texas at Austin

# First-Principles Study of Pockels Effect in Tetragonal $BaTiO_3$

Inhwan Kim

Department of Physics, The University of Texas at Austin

2023 November 13th PMA 11.176

# Magnetic Property

Contents lists available at ScienceDirect

Journal of Alloys and Compounds

journal homepage: www.elsevier.com/locate/jalcom

## Large enhancement of magnetic moment in nitridated $CeFe_{12}$

Joonhyuk Lee[a], Sangkyun Ryu[a], Inhwan Kim[a], Mirang Byeon[b], Myung-Hwan Jeong[c], Jae S. Lee[c], Tae Eun Hong[b], Jinhyung Cho[d], Jaekwang Lee[a,*], Jun Kue Park[c,*], Hyoungjeen Jeen[a,e,*]

[a] Department of Physics, Pusan National University, Busan 46241, South Korea
[b] Busan Center, Korea Basic Science Institute, Busan 46742, South Korea
[c] Korea Multi-Purpose Accelerator Complex, Korea Atomic Energy Research Institute, Gyeongju 38180, South Korea
[d] Department of Physics Education, Pusan National University, Busan 46241 South Korea
[e] Research Center for Dielectric and Advanced Matter Physics, Pusan National University, Busan 46241, South Korea

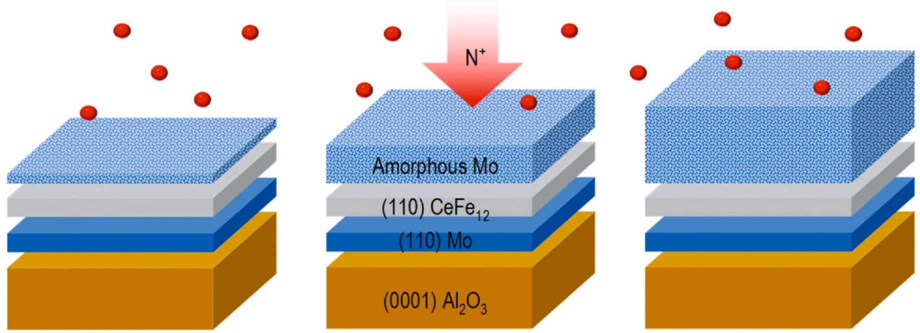


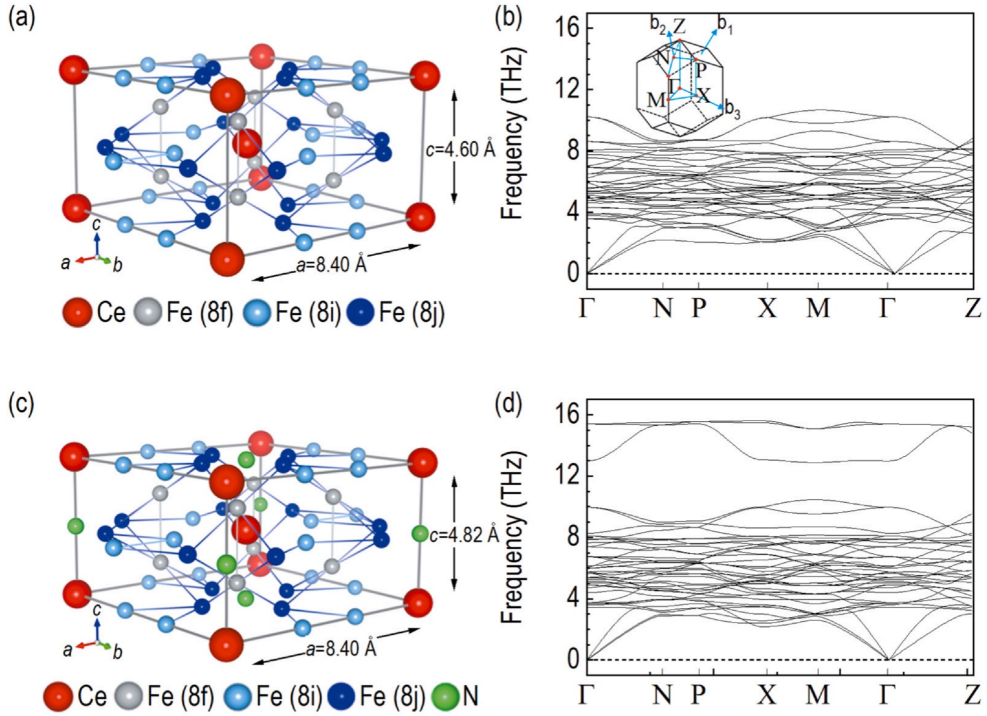


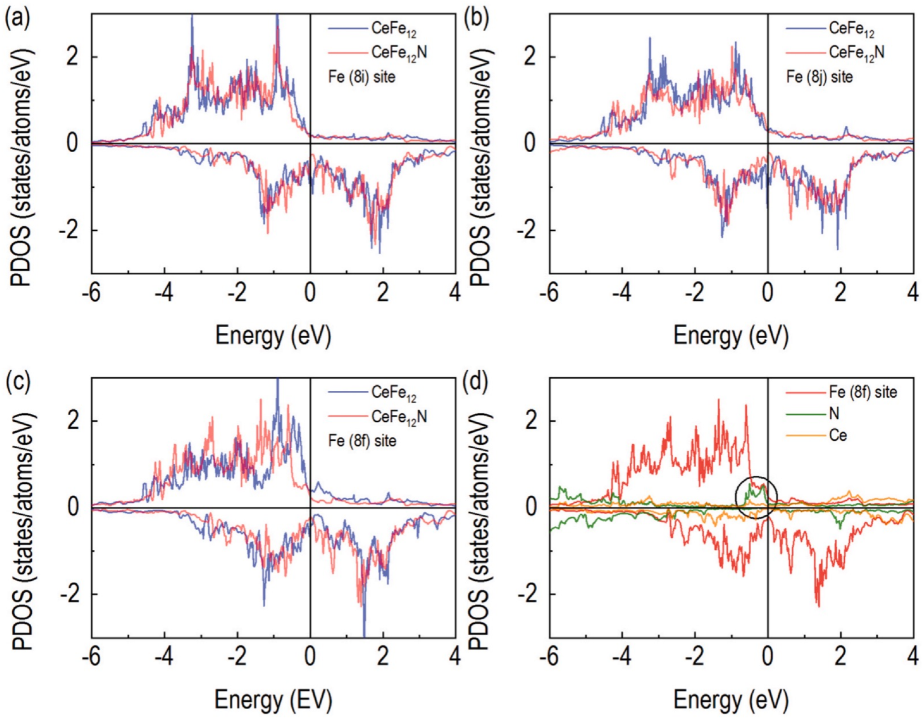

# Dynamics at a phase boundary

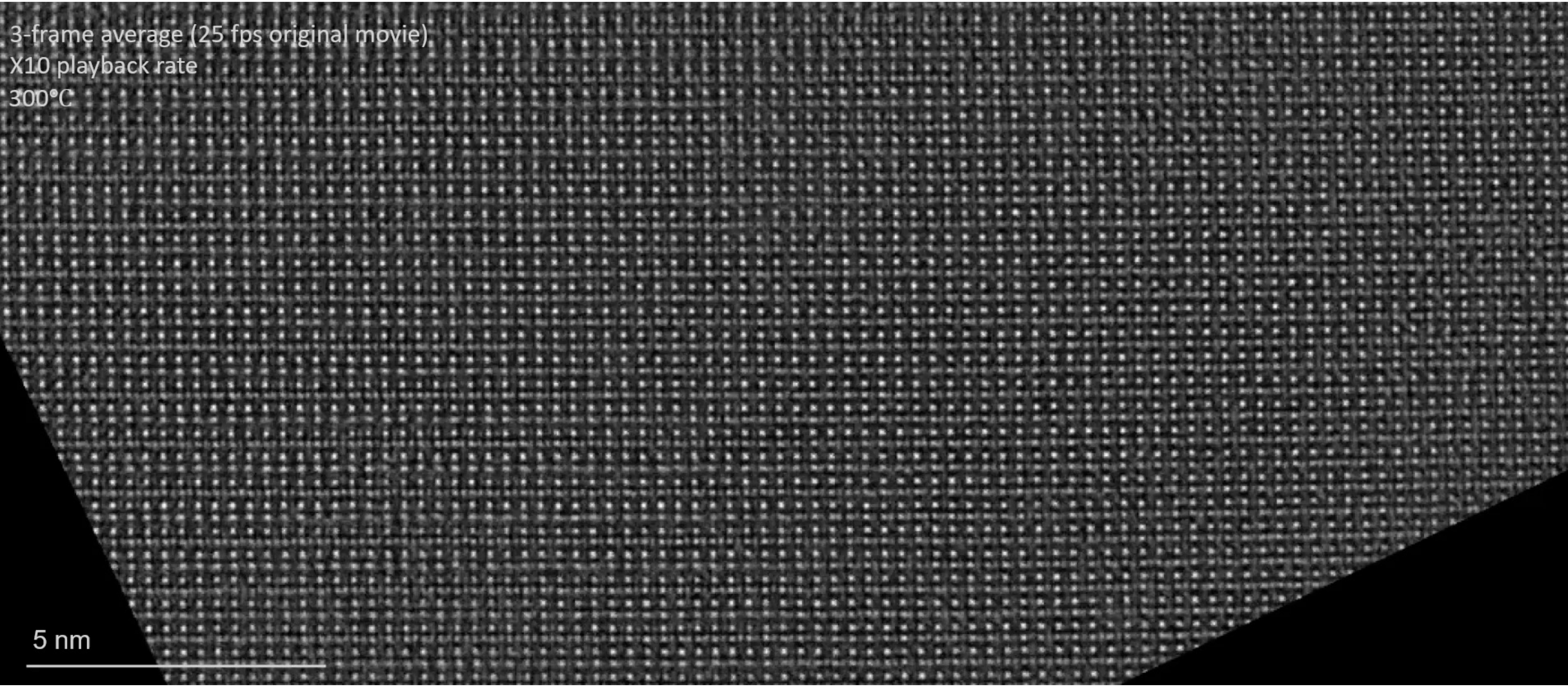

# Dynamics at a phase boundary

Matter
CellPress

Article

## Atomic-scale operando observation of oxygen diffusion during topotactic phase transition of a perovskite oxide

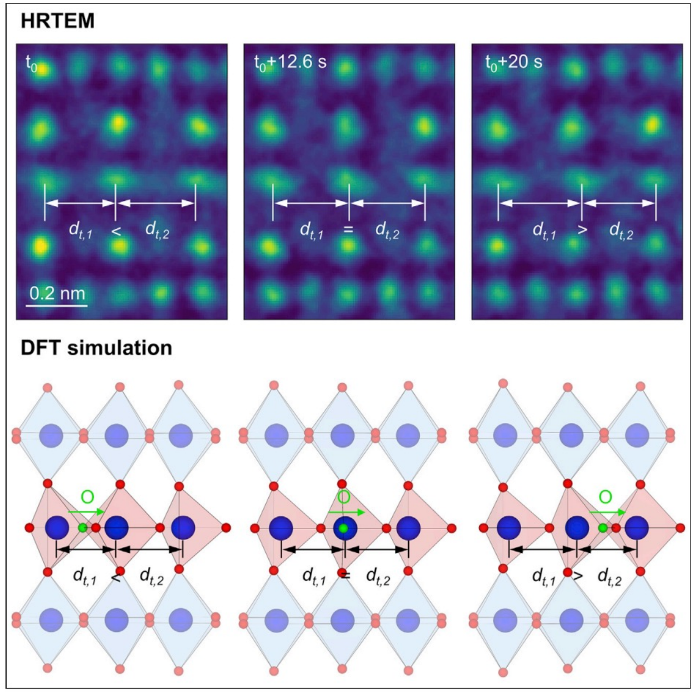


Yaolong Xing, Inhwan Kim, Kyeong Tae Kang, ..., Woo Seok Choi, Jaekwang Lee, Sang Ho Oh

choiws@skku.edu (W.S.C.)
jaekwangl@pusan.ac.kr (J.L.)
shoh@kentech.ac.kr (S.H.O.)

Highlights

Operando atomic-scale imaging of oxygen diffusion during $SrFeO_3$-$SrFeO_{2.5}$ transition

Hyper-stoichiometric $SrFeO_{2.5}$ with excess oxygen emerging at phase boundary

Oxygen diffusion along $FeO_4$ chains via modification of oxygen coordination

Steady-state diffusion via interstitialcy diffusion across fast-diffusion channels

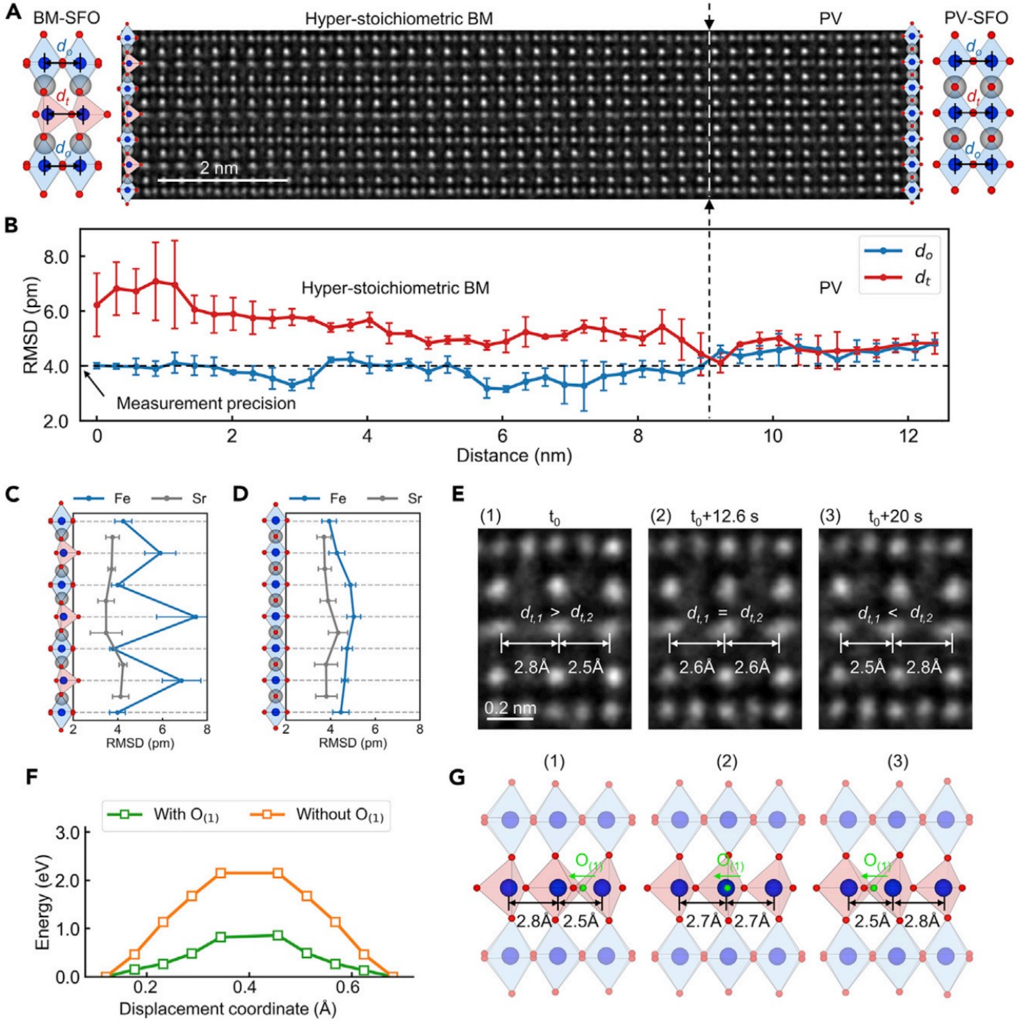

# Linear Electro-Optic response

PHYSICAL REVIEW B **108**, 115201 (2023)

$$= 8\pi\chi^{(2)}_{ij\gamma} + 4\pi\sum_m \frac{1}{\omega_m^2}\left(\sum_{\kappa,\alpha}\frac{\partial\chi^{(1)}_{ij}(\mathbf{R},\eta_0)}{\partial\tau_{\kappa\alpha}}u_m(\kappa\alpha)\right)\times\left(\sum_{\kappa',\beta}Z^*_{\kappa',\gamma\beta}u_m(\kappa'\beta)\right) + p_{ij\mu\nu}d_{\gamma\mu\nu}$$

**Nature of electro-optic response in tetragonal $BaTiO_3$**

Inhwan Kim, Therese Paoletta, and Alexander A. Demkov*

*Department of Physics, The University of Texas, Austin, Texas 78712, USA*

(Received 15 June 2023; revised 7 August 2023; accepted 29 August 2023; published 11 September 2023)

Barium titanate, $BaTiO_3$ (BTO), has emerged as a promising electro-optic material with applications in silicon photonics. It boasts one of the largest known electro-optic coefficients; however, the origin of this giant electro-optic response has not been investigated in detail and is poorly understood. Here we report on a first-principles study of the electro-optic or Pockels tensor in tetragonal *P4mm* BTO. We find good agreement with experiment if the *P4mm* structure is viewed as a dynamic average of four lower symmetry *Cm* structures. The large value of the Raman component of the EO coefficient is attributed to a low frequency and strong electron-phonon coupling of the lowest optical mode, and we trace the equally large piezoelectric contribution to the large components of the piezoelectric and elasto-optic tensors.

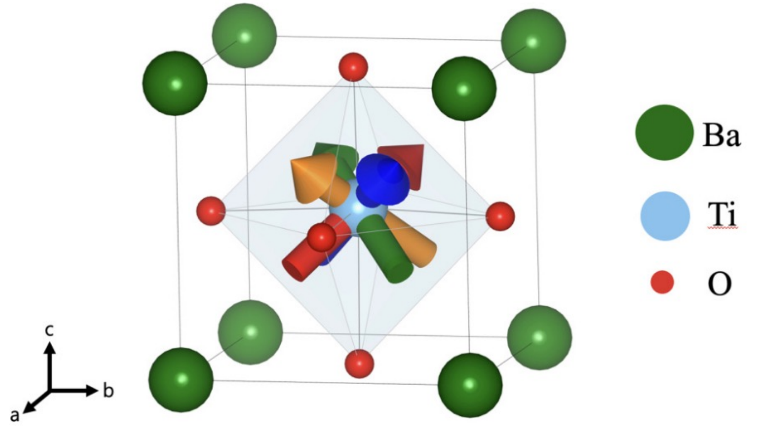


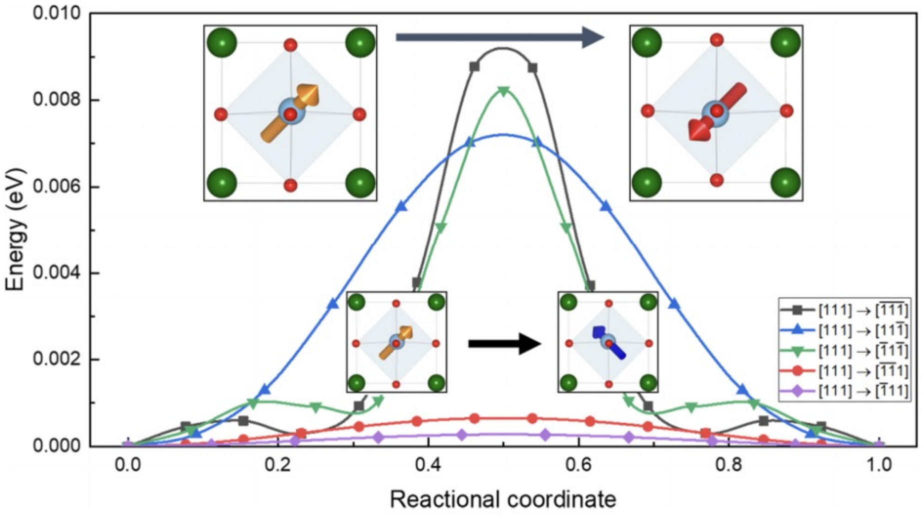


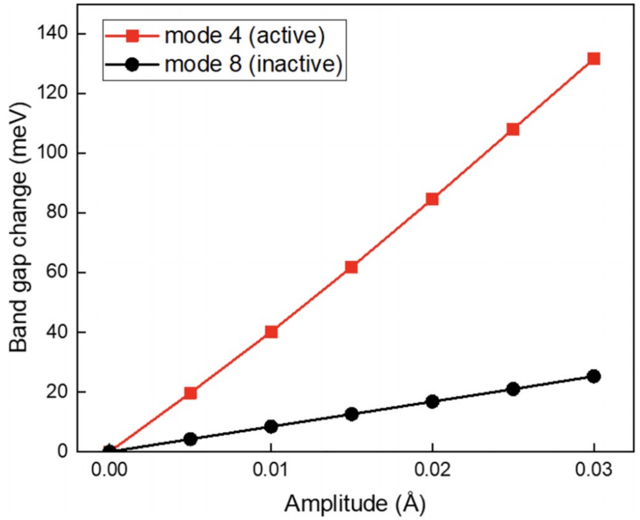


| Electronic Pockels Tensor (pm/V) | | | Ionic Pockels Tensor (pm/V) | | |
|---|---|---|---|---|---|
| 0 | 0 | 0.7 | 1.8 | 0.5 | −25 |
| 0 | 0 | 0.7 | −1.8 | 0.25 | −25 |
| 0 | 0 | 2 | 0 | 0 | 41 |
| 0 | 0.76 | 0 | 0.25 | 823 | 0 |
| 0.76 | 0 | 0 | 816 | 0.5 | 0 |
| 0 | 0 | 0 | 0 | 0 | 0 |

# Linear Electro-Optic response

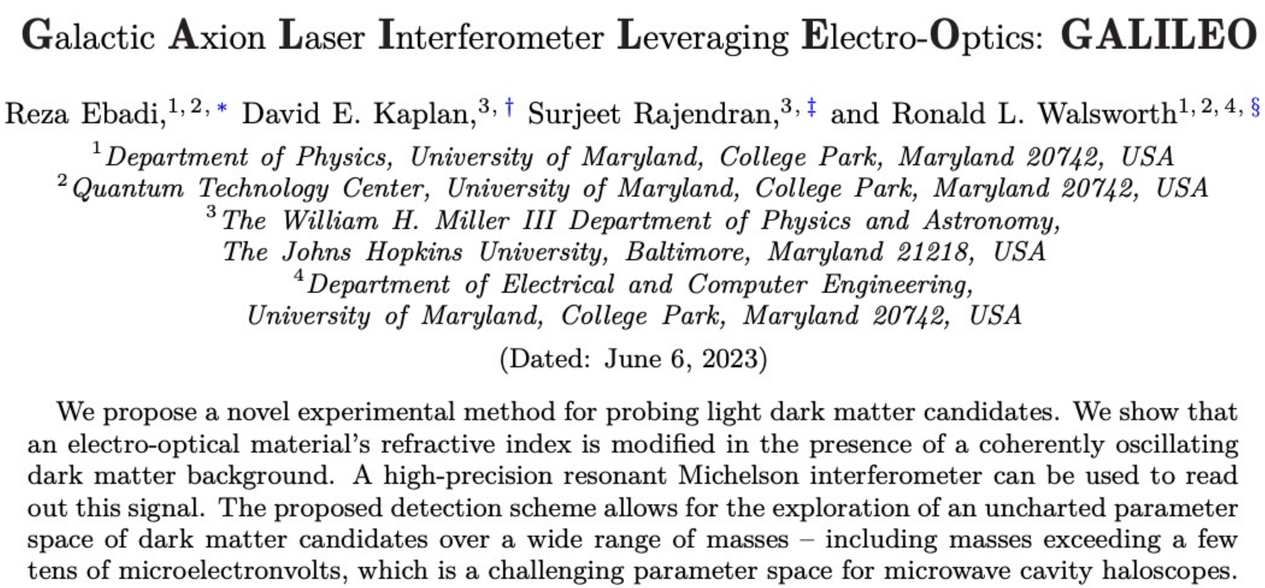

Galactic Axion Laser Interferometer Leveraging Electro-Optics: GALILEO


Reza Ebadi,[1,2,*] David E. Kaplan,[3,†] Surjeet Rajendran,[3,‡] and Ronald L. Walsworth[1,2,4,§]

[1] *Department of Physics, University of Maryland, College Park, Maryland 20742, USA*
[2] *Quantum Technology Center, University of Maryland, College Park, Maryland 20742, USA*
[3] *The William H. Miller III Department of Physics and Astronomy, The Johns Hopkins University, Baltimore, Maryland 21218, USA*
[4] *Department of Electrical and Computer Engineering, University of Maryland, College Park, Maryland 20742, USA*


(Dated: June 6, 2023)


We propose a novel experimental method for probing light dark matter candidates. We show that an electro-optical material's refractive index is modified in the presence of a coherently oscillating dark matter background. A high-precision resonant Michelson interferometer can be used to read out this signal. The proposed detection scheme allows for the exploration of an uncharted parameter space of dark matter candidates over a wide range of masses – including masses exceeding a few tens of microelectronvolts, which is a challenging parameter space for microwave cavity haloscopes.


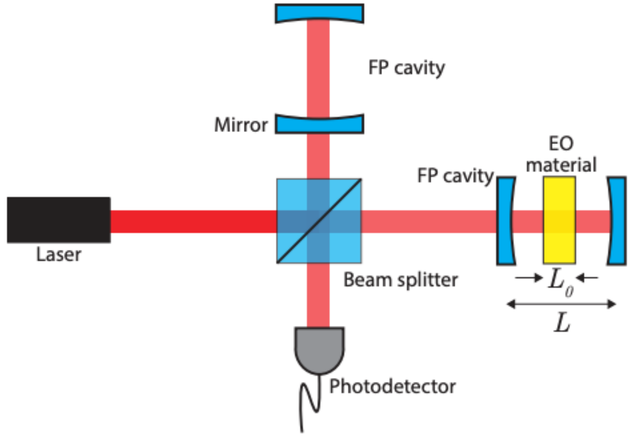


$$\delta n \sim \begin{cases} 1.8 \times 10^{-10}\,(\mathrm{m/V})\ E_{\mathrm{DM}}, & \text{for LiNbO}_3 \\ 6.4 \times 10^{-9}\,(\mathrm{m/V})\ E_{\mathrm{DM}}, & \text{for BaTiO}_3 \end{cases}$$

# And hopefully paper 4 and 5 this year…

MJ10240 - Multiferroism in strained strontium hexaferrite epitaxial thin films

| | |
|---|---|
| **Status:** | With author(s) |
| **Journal:** | Physical Review Materials |
| **Article type:** | Regular Article |
| **Section:** | Magnetic, ferroelectric, and multiferroic materials |
| **Received:** | 05Sep2023 |
| **Author(s):** | Joonhyuk Lee, Sam Yeon Cho, Inhwan Kim, Christopher M. Rouleau, Kungwan Kang, et al. |
| **Corresponding Author:** | Jeen,Hyoung Jeen <hjeen@pusan.ac.kr> |

**manuscript**tracking**system** nature chemistry

tracking system home | submission guidelines | reviewer instructions | help | logout | journal home

### Detailed Status Information

| | |
|---|---|
| **Manuscript #** | NCHEM-23081722 |
| **Current Revision #** | 0 |
| **Submission Date** | 21st August 23 |
| **Current Stage** | Manuscript under consideration |
| **Title** | Formation Mechanism of Infinite-Layer Transition Metal Oxide |
| **Manuscript Type** | Article |

# Outline of the Qualifier Presentation

- Linear electro-optic effect and Silicon photonics
- Tetragonal $BaTiO_3$ as a promising EO material
- Structural consideration
- Clamped Pockels tensor – Ionic contribution
- Unclamped Pockels tensor – Piezo contribution

# Introduction: Silicon Photonics

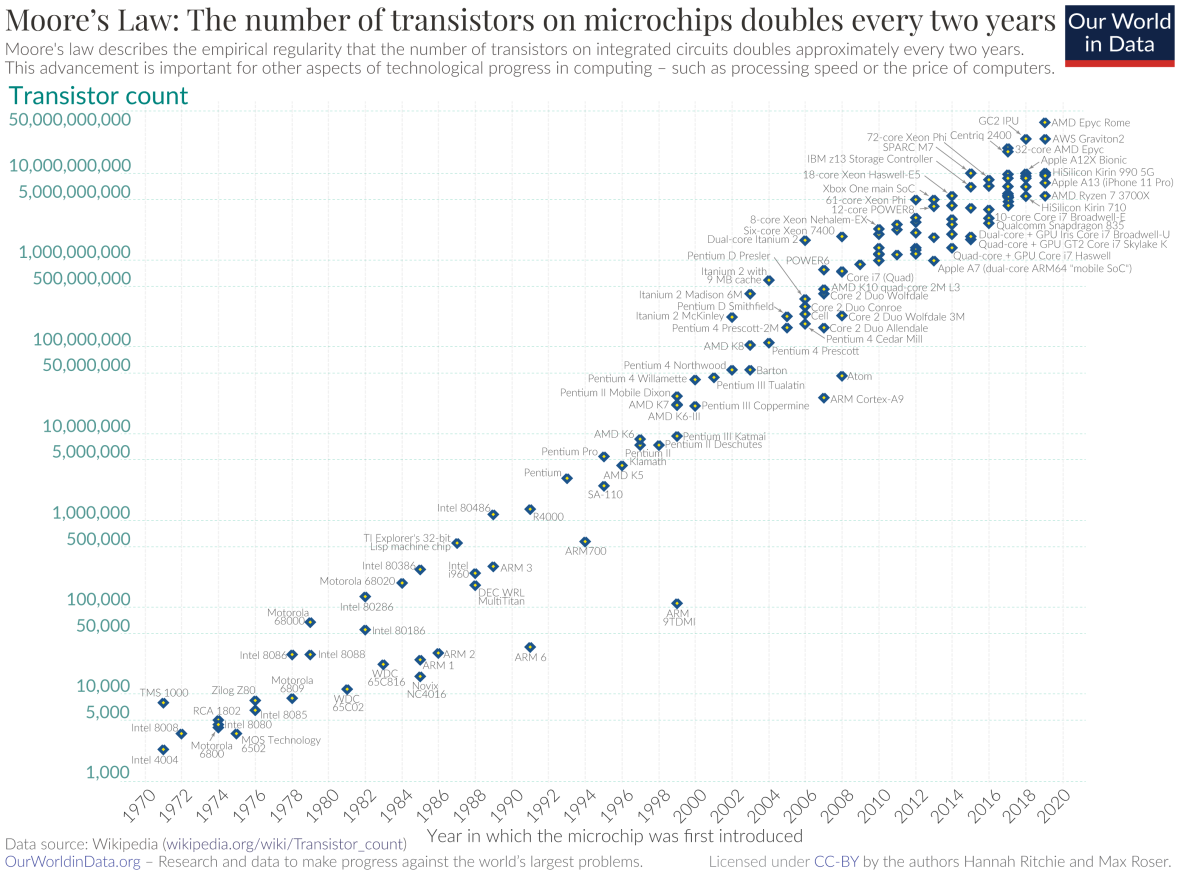


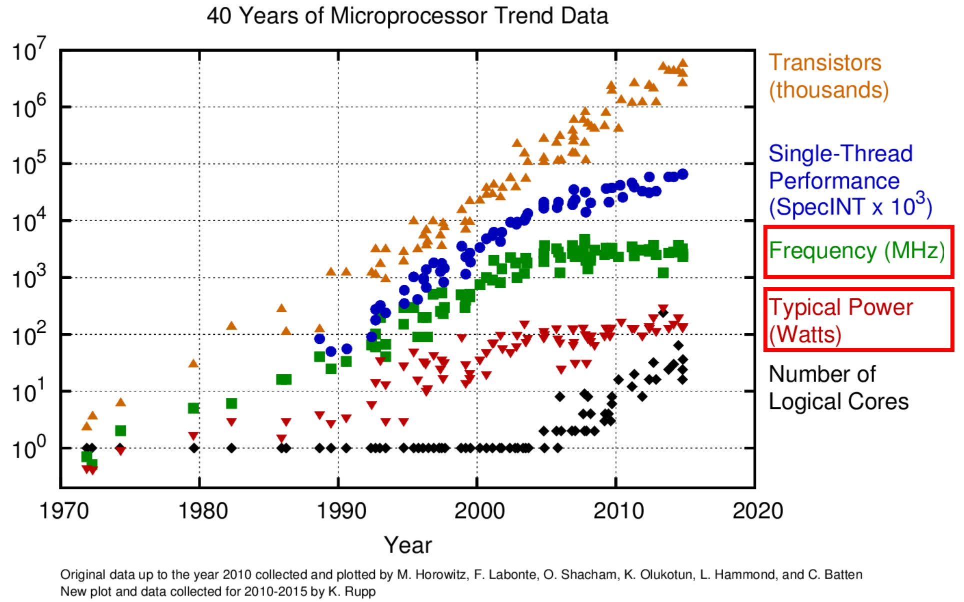


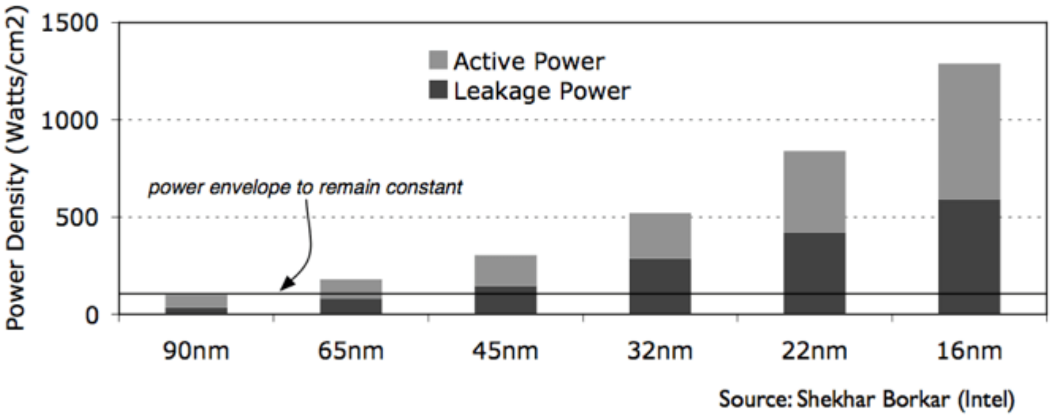


- Moore's law is still working!
- However, both power dissipation and clock speed are currently limiting factors.

# Introduction: Silicon Photonics

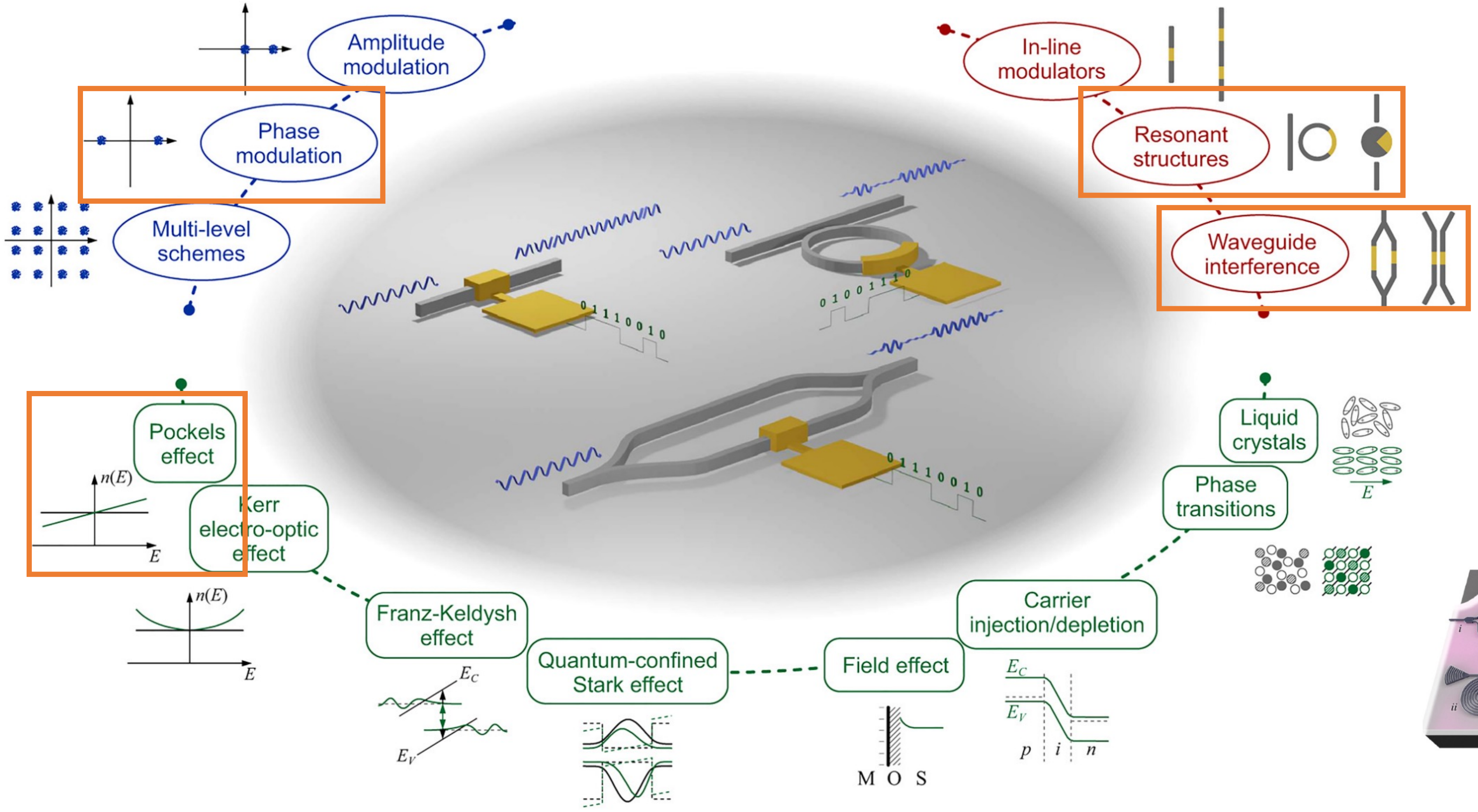


Mach-Zehnder interferometer

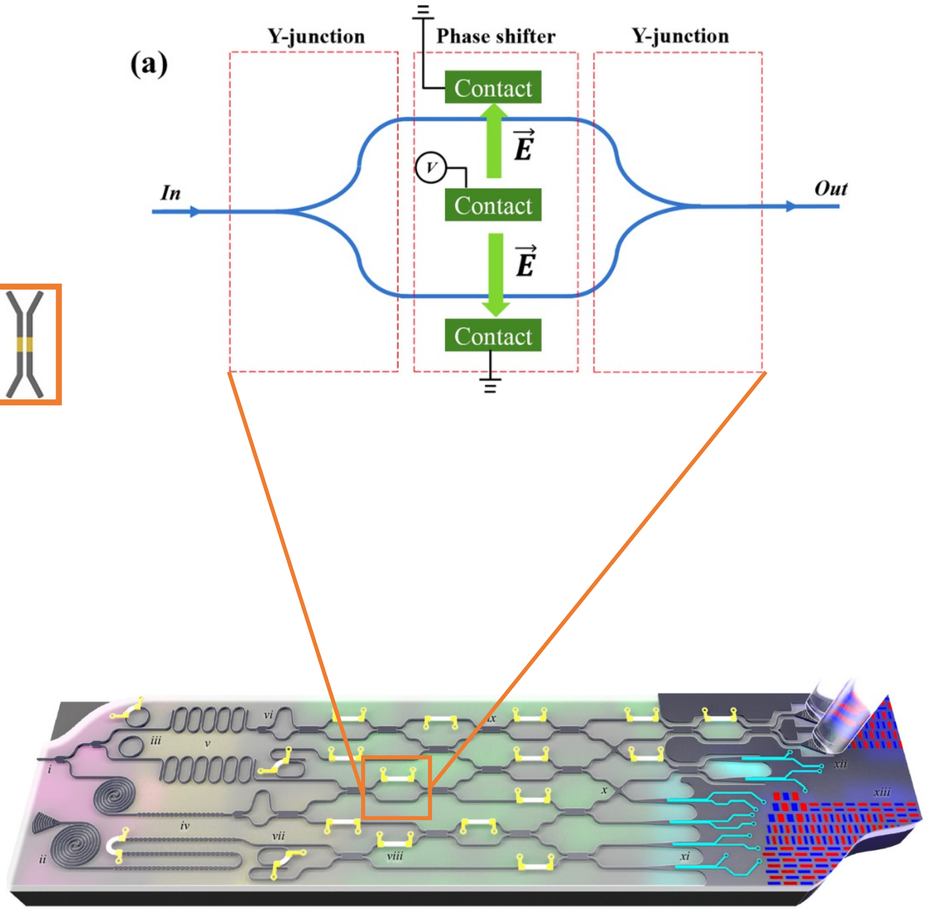


Optical computing in silicon



Demkov *et al.*, J. Appl. Phys. 130, 070907 (2021)
Sinatkas *et al.*, J. Appl. Phys. 130, 010901 (2021)

# Introduction: Electro-Optically Active Materials

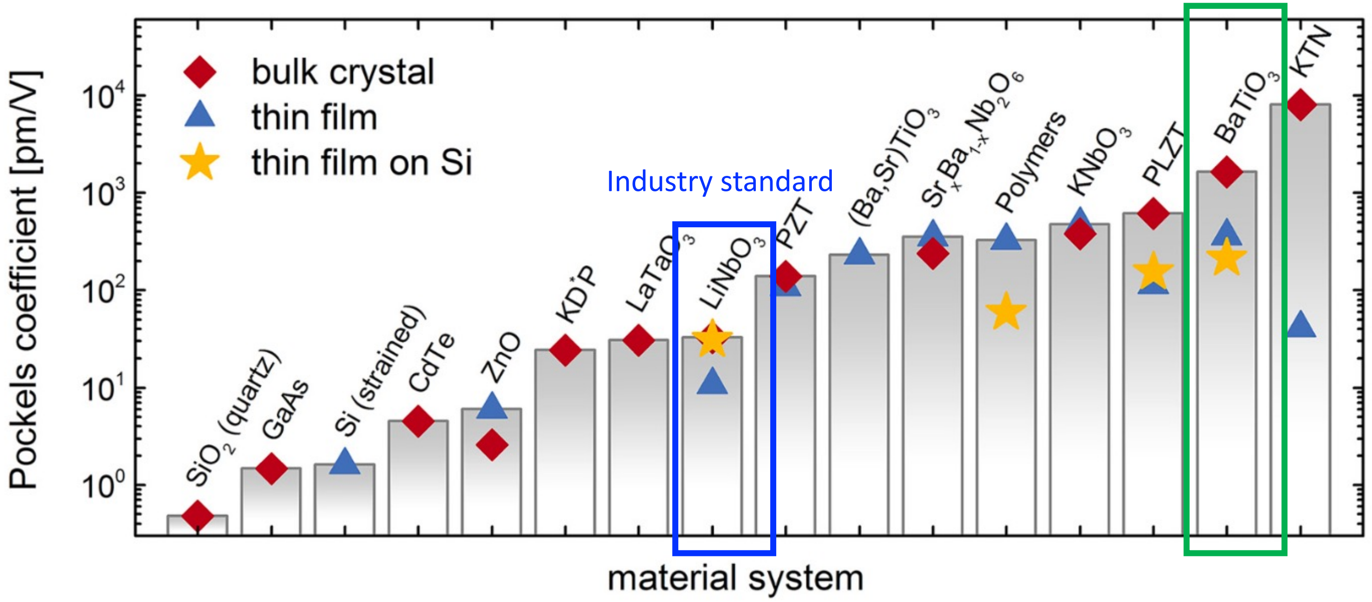


For BTO system

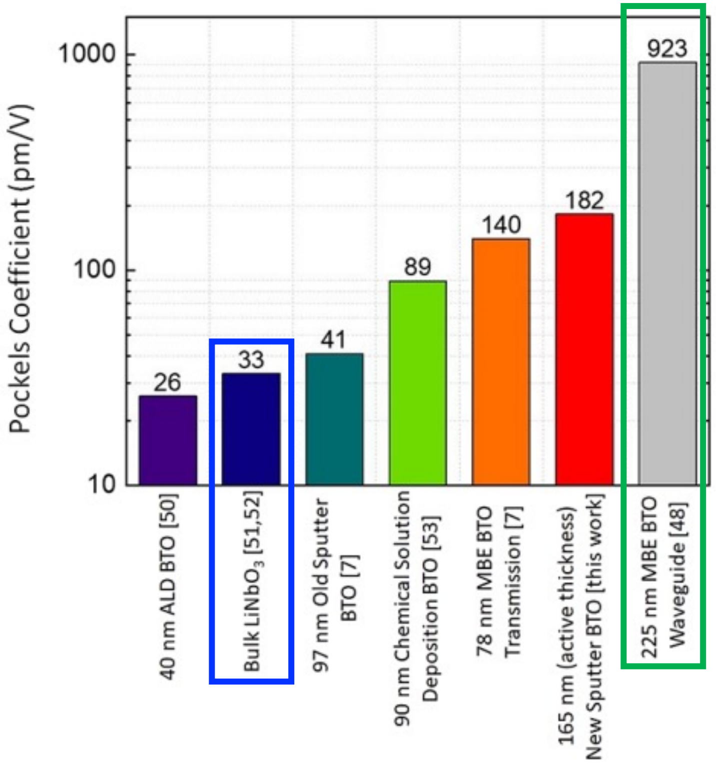


- Bulk tetragonal $BaTiO_3$ is one of the best candidates for the EO material for Si photonics platform
- More theoretical studies are needed to understand the electro-optic properties of BTO



Guo, Demkov *et al.*, J. Vac. Sci. Technol. A 39(3) (2021)
Agham, Demkov *et al*. Appl. Matter. Interfaces 13, 51230 (2021)

# Introduction: Ferroelectric

Displacive type
$BaTiO_3$

Order-disorder type
$LiNbO_3$

- Linear electro-optic effect is only allowed in a crystal without inversion symmetry
- More theoretical studies are needed to understand the electro-optic properties of BTO

# Computational Details

DFT and DFPT calculation:

LDA exchange-correlation with norm-conserving pseudopotentials

For non-linear term, 2n+1 theorem with PEAD formulation

12x12x12 k-point

1000 eV energy cut off

$10^{-5}$ eV/Angstrom

3x3x3 supercell

3x3x3 k-point

Nudged elastic band (NEB) calculation

LO-TO splitting (non-analytical term) is considered

# Self-consistent phonon

Harmonic phonon:
the force acting on atom *l* to *alpha* direction when atom *m* is moved along *beta* direction and all the other atoms are fixed.

$$\Phi_{\alpha\beta}(lm)$$

In contrast, self-consistent phonon:
the force acting on atom *l* should rather be derived by regarding the other atoms as moving. This gives rise to the notion of an effective restoring force. It is defined as a thermodynamical average of the restoring forces, taken over all configurations of the other atoms and weighted with the probability of each configurations.

SCHA is formally again harmonic, the true lattice system is to be approximated by some other effective harmonic lattice whose force constants and lattice parameter are to be optimally adjusted.
The renormalized force constants are obtained from a self-consistency condition. Self-consistency is achieved by replacing the normal harmonic force constants by *effective* force constants which are thermal averages with respect to the *effective* harmonic Hamiltonian.

# The Linear Electro-Optic Response: the Pockels Effect

$$\Delta\left(\frac{1}{n^2}\right) = \Delta\left(\varepsilon^{-1}\right)_{ij} = \sum_{\gamma} r_{ij\gamma} E_{\gamma}$$

$$\Delta\left(\varepsilon^{-1}\right)_{ij} = -\varepsilon_{im}^{(-1)} \Delta\varepsilon_{mn} \varepsilon_{nj}^{(-1)}$$



Veithen, Gonze, Ghosez, Phys. Rev. Lett. 93, 187401 (2004)
Veithen , Gonze, Ghosez, Phys. Rev. B. 71, 125107 (2005)

# The Linear Electro-Optic Response: the Pockels Effect

$$\Delta\left(\frac{1}{n^2}\right) = \Delta\left(\varepsilon^{-1}\right)_{ij} = \sum_{\gamma} \underbrace{r_{ij\gamma}}_{\text{Pockels tensor}} E_{\gamma}$$

$$\Delta\left(\varepsilon^{-1}\right)_{ij} = -\varepsilon_{im}^{(-1)} \Delta\varepsilon_{mn} \varepsilon_{nj}^{(-1)}$$

$$\begin{aligned}
\left[\frac{d\varepsilon_{ij}(\mathbf{R},\eta_0,E)}{dE_\gamma}\right]_{\mathbf{R}_0,\eta_0,E=0} &= \left[\frac{\partial\varepsilon_{ij}(\mathbf{R},\eta_0,E)}{\partial E_\gamma}\right]_{E=0} + \left[\frac{\partial\varepsilon_{ij}(\mathbf{R},\eta_0,E)}{\partial\tau_{\kappa\alpha}}\right]_{\mathbf{R}_0} \frac{\partial\tau_{\kappa\alpha}}{\partial E_\gamma} + \left[\frac{\partial\varepsilon_{ij}(\mathbf{R},\eta_0,E)}{\partial\eta_{\mu\nu}}\right]_{\eta_0} \frac{\partial\eta_{\mu\nu}}{\partial E_\gamma} \\
&= 8\pi\chi_{ij\gamma}^{(2)} + 4\pi\sum_m \underbrace{\frac{1}{\omega_m^2}}_{\text{Phonon}} \underbrace{\left(\sum_{\kappa,\alpha}\frac{\partial\chi_{ij}^{(1)}(\mathbf{R},\eta_0)}{\partial\tau_{\kappa\alpha}} u_m(\kappa\alpha)\right)}_{\text{Raman susceptibility tensor}} \times \underbrace{\left(\sum_{\kappa',\beta} Z^*_{\kappa',\gamma\beta} u_m(\kappa'\beta)\right)}_{\text{Mode polarity}} + \underbrace{p_{ij\mu\nu}}_{\text{Elasto-optic tensor}} \overbrace{d_{\gamma\mu\nu}}^{\text{Piezoelectric tensor}} \\
&= \underbrace{r_{ij\gamma}^{elec} + r_{ij\gamma}^{ion} + r_{ij\gamma}^{piezo}}_{\text{Unclamped EO tensor}}.
\end{aligned}$$



Veithen, Gonze, Ghosez, Phys. Rev. Lett. 93, 187401 (2004)
Veithen , Gonze, Ghosez, Phys. Rev. B. 71, 125107 (2005)

# The Linear Electro-Optic Response: the Pockels Effect

Electric enthalpy is defined as,

$$F(\mathbf{r},\eta,\mathbf{E}) = F(\mathbf{r},\eta,\mathbf{E}=0) - \Omega_0 P_i(\mathbf{R},\eta)E_i - \frac{\Omega_0}{8\pi}\varepsilon_{ij}(\mathbf{R},\eta)E_iE_j - \frac{\Omega_0}{3}\chi^{(2)}_{ijk}(\mathbf{R},\eta)E_iE_jE_k + \cdots$$

$$\frac{\partial F}{\partial \tau_{\kappa\alpha}} = 0$$ : The equilibrium condition of electric enthalpy F

$$= \left.\frac{\partial F(\mathbf{R},\eta_0,\mathbf{E}=0)}{\partial \tau_{\kappa\alpha}}\right|_{\mathbf{R}(E)} - \Omega_0 \left.\frac{\partial P_i(\mathbf{R},\eta_0)}{\partial \tau_{\kappa\alpha}}\right|_{\mathbf{R}(E)} E_i - \frac{\Omega_0}{8\pi}\left.\frac{\partial \varepsilon_{ij}(\mathbf{R},\eta_0)}{\partial \tau_{\kappa\alpha}}\right|_{\mathbf{R}(E)} E_iE_j + \cdots$$

$$\left.\frac{\partial^2 F(\mathbf{R},\eta_0,\mathbf{E}=0)}{\partial \tau_{\kappa\alpha}\partial \tau_{\kappa'\alpha'}}\right|_{\mathbf{R}_0} \frac{\partial \tau_{\kappa'\alpha'}}{\partial E_\gamma} = \Omega_0 \left.\frac{\partial P_\gamma(\mathbf{R},\eta_0)}{\partial \tau_{\kappa\alpha}}\right|_{\mathbf{R}_0} \qquad \tau_{\kappa\alpha} = \tau_m u_m(\kappa\alpha) \quad \Rightarrow \quad \boxed{\frac{\partial \tau_m}{\partial E_\gamma} = \frac{1}{\omega_m^2}\sum_{\kappa,\alpha} Z^*_{\kappa,\gamma\alpha} u_m(\kappa\alpha)}$$

# The Linear Electro-Optic Response: the Pockels Effect

$$\left[\frac{d\varepsilon_{ij}(\mathbf{R},\eta_0,E)}{dE_\gamma}\right]_{\mathbf{R}_0,\eta_0,E=0} = 8\pi\chi^{(2)}_{ij\gamma} + 4\pi\sum_m \underbrace{\frac{1}{\omega_m^2}}_{\text{Phonon}} \underbrace{\left(\sum_{\kappa,\alpha}\frac{\partial\chi^{(1)}_{ij}(\mathbf{R},\eta_0)}{\partial\tau_{\kappa\alpha}}u_m(\kappa\alpha)\right)}_{\text{Raman susceptibility tensor}} \times \underbrace{\left(\sum_{\kappa',\beta} Z^*_{\kappa',\gamma\beta}u_m(\kappa'\beta)\right)}_{\text{Mode polarity}} + \underbrace{p_{ij\mu\nu}}_{\text{Elasto-optic tensor}}\overbrace{d_{\gamma\mu\nu}}^{\text{Piezoelectric tensor}}$$

$$= \underbrace{r^{elec}_{ij\gamma} + r^{ion}_{ij\gamma} + r^{piezo}_{ij\gamma}}_{\text{Unclamped EO tensor}}.$$



Veithen, Gonze, Ghosez, Phys. Rev. Lett. 93, 187401 (2004)
Veithen , Gonze, Ghosez, Phys. Rev. B. 71, 125107 (2005)

# Phonon part

$$4\pi \sum_m \underline{\frac{1}{\omega_m^2}}$$

Phonon

$$\underline{u_m(\kappa\alpha)}$$

eigendisplacement



Veithen, Gonze, Ghosez, Phys. Rev. Lett. 93, 187401 (2004)
Veithen , Gonze, Ghosez, Phys. Rev. B. 71, 125107 (2005)

# Phonon part

$$\left[\frac{d\varepsilon_{ij}(\mathbf{R},\eta_0,E)}{dE_\gamma}\right]_{\mathbf{R}_0,\eta_0,E=0} = 8\pi\chi^{(2)}_{ij\gamma} + 4\pi\sum_m \underbrace{\frac{1}{\omega_m^2}}_{\text{Phonon}} \underbrace{\left(\sum_{\kappa,\alpha}\frac{\partial\chi^{(1)}_{ij}(\mathbf{R},\eta_0)}{\partial\tau_{\kappa\alpha}}u_m(\kappa\alpha)\right)}_{\text{Raman susceptibility tensor}} \times \underbrace{\left(\sum_{\kappa',\beta} Z^*_{\kappa',\gamma\beta}u_m(\kappa'\beta)\right)}_{\text{Mode polarity}} + \underbrace{p_{ij\mu\nu}}_{\text{Elasto-optic tensor}}\overbrace{d_{\gamma\mu\nu}}^{\text{Piezoelectric tensor}}$$

$$= \underbrace{r^{elec}_{ij\gamma}+r^{ion}_{ij\gamma}+r^{piezo}_{ij\gamma}}_{\text{Unclamped EO tensor}}.$$



Veithen, Gonze, Ghosez, Phys. Rev. Lett. 93, 187401 (2004)
Veithen , Gonze, Ghosez, Phys. Rev. B. 71, 125107 (2005)

# Raman susceptibility part

$$\underbrace{\left(\sum_{\kappa,\alpha}\frac{\partial\chi^{(1)}_{ij}(\mathbf{R},\eta_0)}{\partial\tau_{\kappa\alpha}}u_m(\kappa\alpha)\right)}_{\text{Raman susceptibility tensor}}$$



Veithen, Gonze, Ghosez, Phys. Rev. Lett. 93, 187401 (2004)
Veithen , Gonze, Ghosez, Phys. Rev. B. 71, 125107 (2005)

# Mode polarity part

$$\left[\frac{d\varepsilon_{ij}(\mathbf{R},\eta_0,E)}{dE_\gamma}\right]_{\mathbf{R}_0,\eta_0,E=0} = 8\pi\chi^{(2)}_{ij\gamma} + 4\pi\sum_m \underbrace{\frac{1}{\omega_m^2}}_{\text{Phonon}} \underbrace{\left(\sum_{\kappa,\alpha}\frac{\partial\chi^{(1)}_{ij}(\mathbf{R},\eta_0)}{\partial\tau_{\kappa\alpha}}u_m(\kappa\alpha)\right)}_{\text{Raman susceptibility tensor}} \times \underbrace{\left(\sum_{\kappa',\beta}Z^*_{\kappa',\gamma\beta}u_m(\kappa'\beta)\right)}_{\text{Mode polarity}} + \underbrace{p_{ij\mu\nu}}_{\text{Elasto-optic tensor}}\overbrace{d_{\gamma\mu\nu}}^{\text{Piezoelectric tensor}}$$

$$= \underbrace{r^{elec}_{ij\gamma} + r^{ion}_{ij\gamma} + r^{piezo}_{ij\gamma}}_{\text{Unclamped EO tensor}}.$$



Veithen, Gonze, Ghosez, Phys. Rev. Lett. 93, 187401 (2004)
Veithen , Gonze, Ghosez, Phys. Rev. B. 71, 125107 (2005)

# Piezoelectric part

$$\left[\frac{d\varepsilon_{ij}(\mathbf{R},\eta_0,E)}{dE_\gamma}\right]_{\mathbf{R}_0,\eta_0,E=0} = 8\pi\chi^{(2)}_{ij\gamma} + 4\pi\sum_m \underbrace{\frac{1}{\omega_m^2}}_{\text{Phonon}} \underbrace{\left(\sum_{\kappa,\alpha}\frac{\partial\chi^{(1)}_{ij}(\mathbf{R},\eta_0)}{\partial\tau_{\kappa\alpha}}u_m(\kappa\alpha)\right)}_{\text{Raman susceptibility tensor}} \times \underbrace{\left(\sum_{\kappa',\beta} Z^*_{\kappa',\gamma\beta}u_m(\kappa'\beta)\right)}_{\text{Mode polarity}} + \underbrace{p_{ij\mu\nu}}_{\text{Elasto-optic tensor}}\overbrace{d_{\gamma\mu\nu}}^{\text{Piezoelectric tensor}}$$

$$= \underbrace{r^{elec}_{ij\gamma} + r^{ion}_{ij\gamma} + r^{piezo}_{ij\gamma}}_{\text{Unclamped EO tensor}}.$$



Veithen, Gonze, Ghosez, Phys. Rev. Lett. 93, 187401 (2004)
Veithen , Gonze, Ghosez, Phys. Rev. B. 71, 125107 (2005)

# Elasto-optic part

$$\left[\frac{d\varepsilon_{ij}(\mathbf{R},\eta_0,E)}{dE_\gamma}\right]_{\mathbf{R}_0,\eta_0,E=0} = 8\pi\chi^{(2)}_{ij\gamma} + 4\pi\sum_m \underbrace{\frac{1}{\omega_m^2}}_{\text{Phonon}} \underbrace{\left(\sum_{\kappa,\alpha}\frac{\partial\chi^{(1)}_{ij}(\mathbf{R},\eta_0)}{\partial\tau_{\kappa\alpha}}u_m(\kappa\alpha)\right)}_{\text{Raman susceptibility tensor}} \times \underbrace{\left(\sum_{\kappa',\beta}Z^*_{\kappa',\gamma\beta}u_m(\kappa'\beta)\right)}_{\text{Mode polarity}} + \underbrace{p_{ij\mu\nu}}_{\text{Elasto-optic tensor}}\overbrace{d_{\gamma\mu\nu}}^{\text{Piezoelectric tensor}}$$

$$= \underbrace{r^{elec}_{ij\gamma} + r^{ion}_{ij\gamma} + r^{piezo}_{ij\gamma}}_{\text{Unclamped EO tensor}}.$$



Veithen, Gonze, Ghosez, Phys. Rev. Lett. 93, 187401 (2004)
Veithen , Gonze, Ghosez, Phys. Rev. B. 71, 125107 (2005)

# Pockels response in rhombohedral $BaTiO_3$

$$4\pi \sum_m \boxed{\frac{1}{\omega_m^2}} \left( \sum_{\kappa,\alpha} \frac{\partial \chi_{ij}^{(1)}(\mathbf{R}, \eta_0)}{\partial \tau_{\kappa\alpha}} u_m(\kappa\alpha) \right) \times \left( \sum_{\kappa',\beta} Z^*_{\kappa',\gamma\beta} u_m(\kappa'\beta) \right)$$

Imaginary!

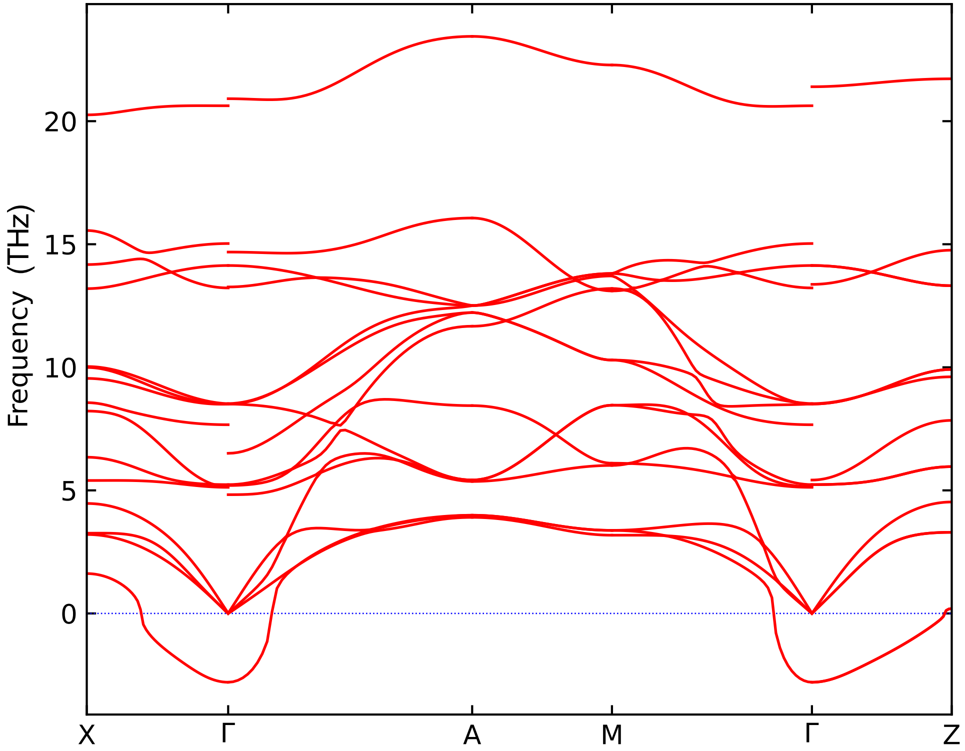


Imaginary phonon modes in the *P4mm* phase make the calculation difficult

# Structural Problem: imaginary phonon mode in *P4mm* $BaTiO_3$

$$4\pi \sum_m \boxed{\frac{1}{\omega_m^2}} \left( \sum_{\kappa,\alpha} \frac{\partial \chi_{ij}^{(1)}(\mathbf{R}, \eta_0)}{\partial \tau_{\kappa\alpha}} u_m(\kappa\alpha) \right) \times \left( \sum_{\kappa',\beta} Z^*_{\kappa',\gamma\beta} u_m(\kappa'\beta) \right)$$

Imaginary!

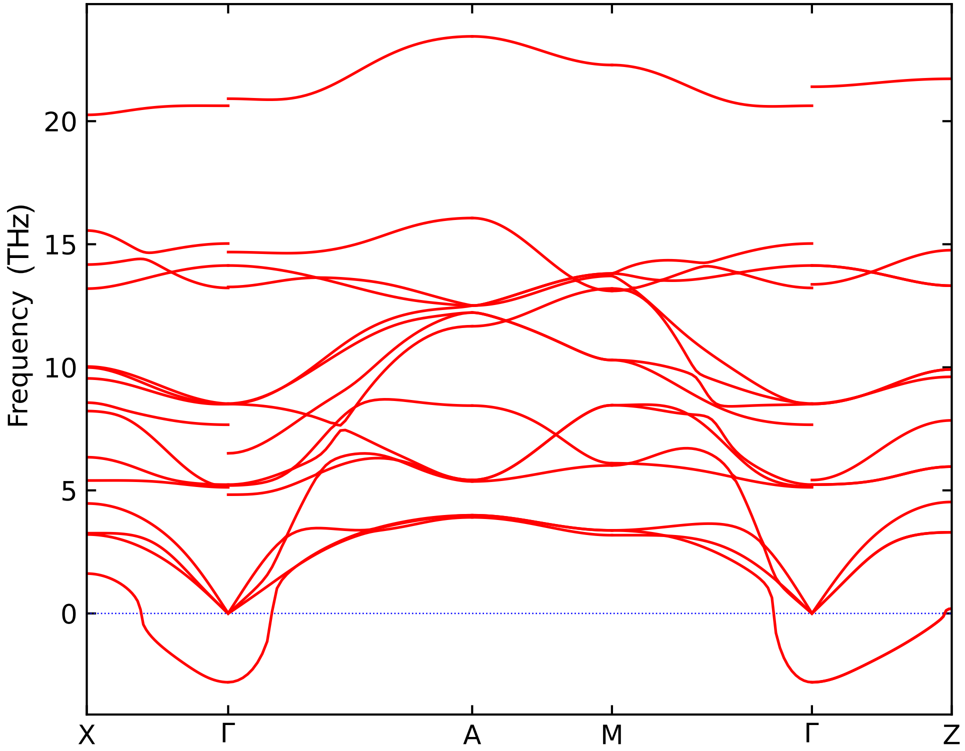


Imaginary phonon modes in the *P4mm* phase make the calculation difficult

# Structural Problem: *P4mm* as average *Cm* structure

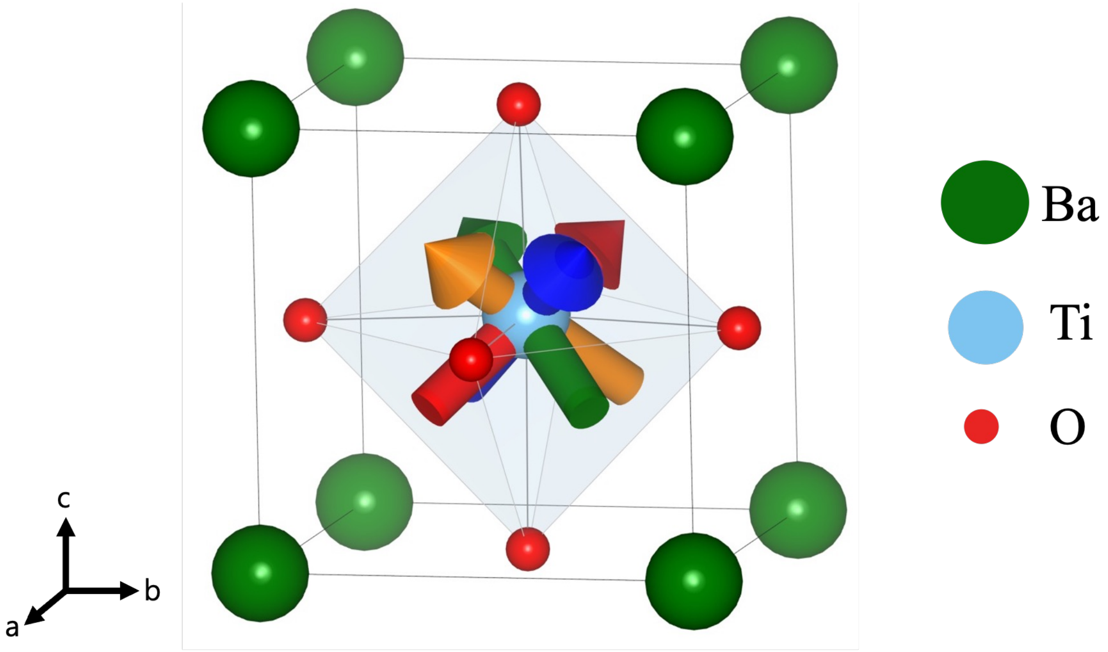


Other experiment results from the other presentations by Dr. Kotiuga

- In recent experiments, the high symmetry structures are microscopically averaged over low-symmetry phase
- We assume our tetragonal structure is microscopically averaged over [111]-displacement.



Senn *et al.*, Phys. Rev. Lett. 116, 207602 (2016)
Tsuda *et al.*, Appl. Phys. Express 9, 071501 (2016)

# Structural Problem: *P4mm* as average *Cm* structure

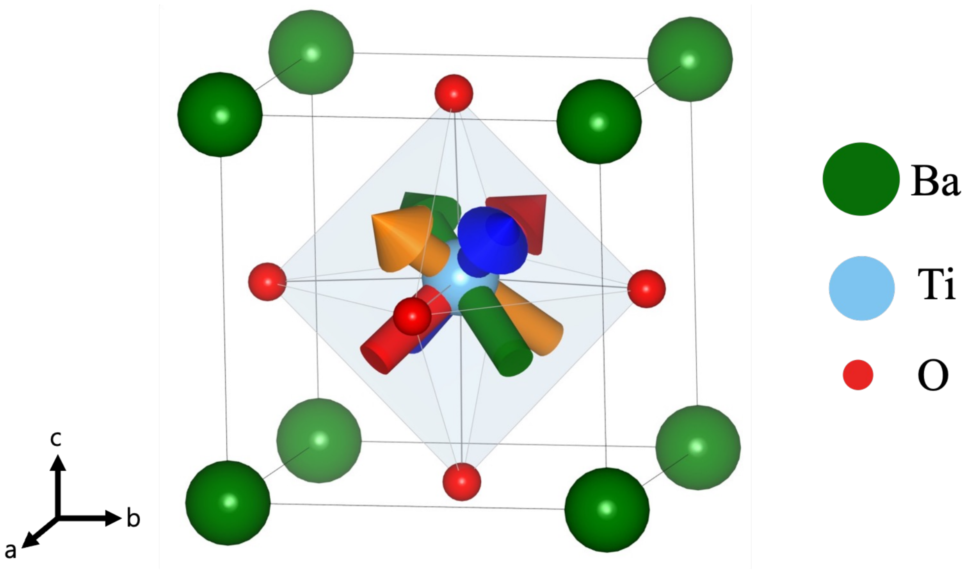


| | *P4mm* | | | *Cm* | | |
|---|---|---|---|---|---|---|
| Element | x | Y | z | x | y | z |
| Ba | 0 | 0 | 0 | 0 | 0 | 0 |
| Ti | 0.5 | 0.5 | 0.513 | 0.507 | 0.507 | 0.513 |
| $O_1$ | 0 | 0.5 | 0.487 | 0 | 0.494 | 0.488 |
| $O_2$ | 0.5 | 0 | 0.487 | 0.494 | 0 | 0.488 |
| $O_3$ | 0.5 | 0.5 | 0.98 | 0.495 | 0.495 | 0.981 |

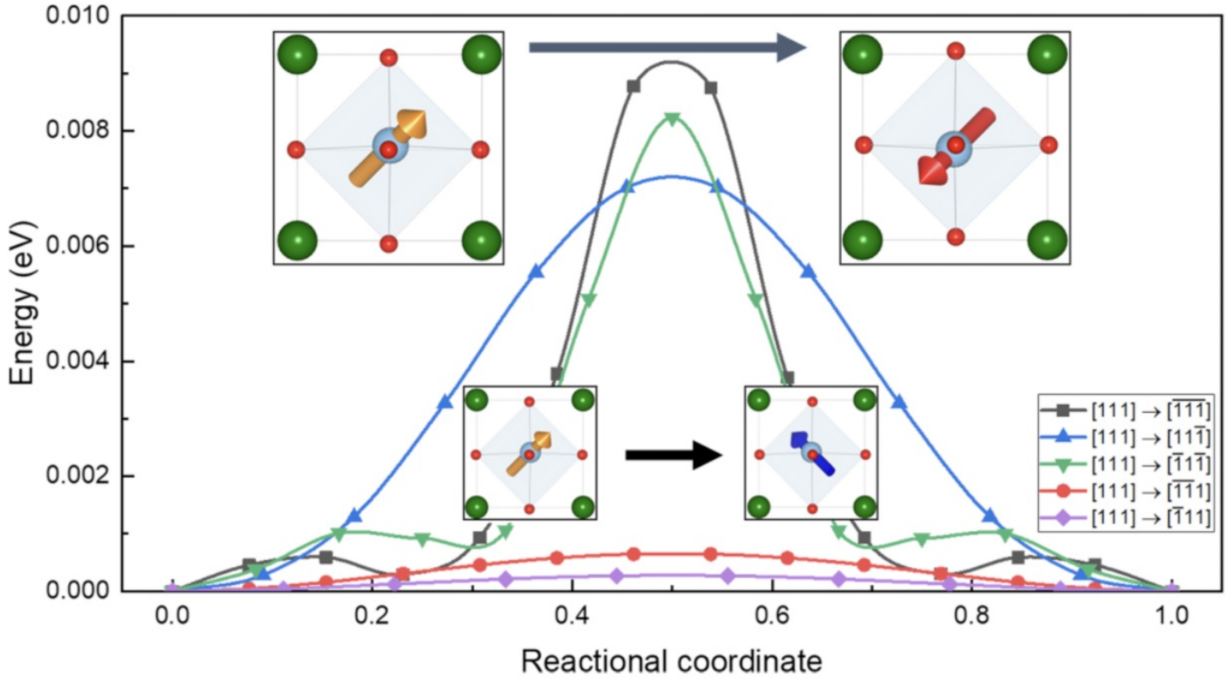


- In experiments, the *P4mm* tetragonal structure is microscopically averaged over [111]-displacement.
- Energy barrier is much higher to flip the macroscopic polarization direction.



Senn *et al.*, Phys. Rev. Lett. 116, 207602 (2016)
Tsuda *et al.*, Appl. Phys. Express 9, 071501 (2016)

# Ionic Electro-Optic Response: Phonon

$$4\pi \sum_m \boxed{\frac{1}{\omega_m^2}} \left( \sum_{\kappa,\alpha} \frac{\partial \chi_{ij}^{(1)}(\mathbf{R},\eta_0)}{\partial \tau_{\kappa\alpha}} u_m(\kappa\alpha) \right) \times \left( \sum_{\kappa',\beta} Z^*_{\kappa',\gamma\beta} u_m(\kappa'\beta) \right)$$

| Mode Number | *P4mm* SR ($cm^{-1}$) | *P4mm* LR ($cm^{-1}$) | *Cm* SR ($cm^{-1}$) | *Cm* LR ($cm^{-1}$) | SCPH ($cm^{-1}$) | Exp. [54] ($cm^{-1}$) |
|---|---|---|---|---|---|---|
| 4 | $-176\,i$ | $-176\,i$ | 17 | 57 | 161 | 34 |
| 5 | $-176\,i$ | $-176\,i$ | 78 | 170 | 171 | 180 |
| 6 | 164 | 170 | 170 | 174 | 174 | 189 |
| 7 | 170 | 170 | 174 | 175 | 174 | |
| 8 | 170 | 185 | 175 | 235 | 264 | |
| 9 | 287 | 287 | 236 | 284 | 281 | |
| 10 | 287 | 287 | 284 | 294 | 281 | 304 |
| 11 | 291 | 291 | 294 | 296 | 282 | 308 |
| 12 | 315 | 453 | 295 | 452 | 465 | 471 |
| 13 | 457 | 457 | 471 | 472 | 490 | 498 |
| 14 | 457 | 457 | 471 | 492 | 510 | |
| 15 | 515 | 718 | 495 | 674 | 710 | 725 |

NO imaginary values

# Ionic Electro-Optic Response: Raman and Mode Polarity

$$4\pi \sum_m \frac{1}{\omega_m^2} \underbrace{\left( \sum_{\kappa,\alpha} \frac{\partial \chi_{ij}^{(1)}(\mathbf{R}, \eta_0)}{\partial \tau_{\kappa\alpha}} u_m(\kappa\alpha) \right)}_{\text{Raman susceptibility tensor}} \times \underbrace{\left( \sum_{\kappa',\beta} Z^*_{\kappa',\gamma\beta} u_m(\kappa'\beta) \right)}_{\text{Mode polarity}}$$

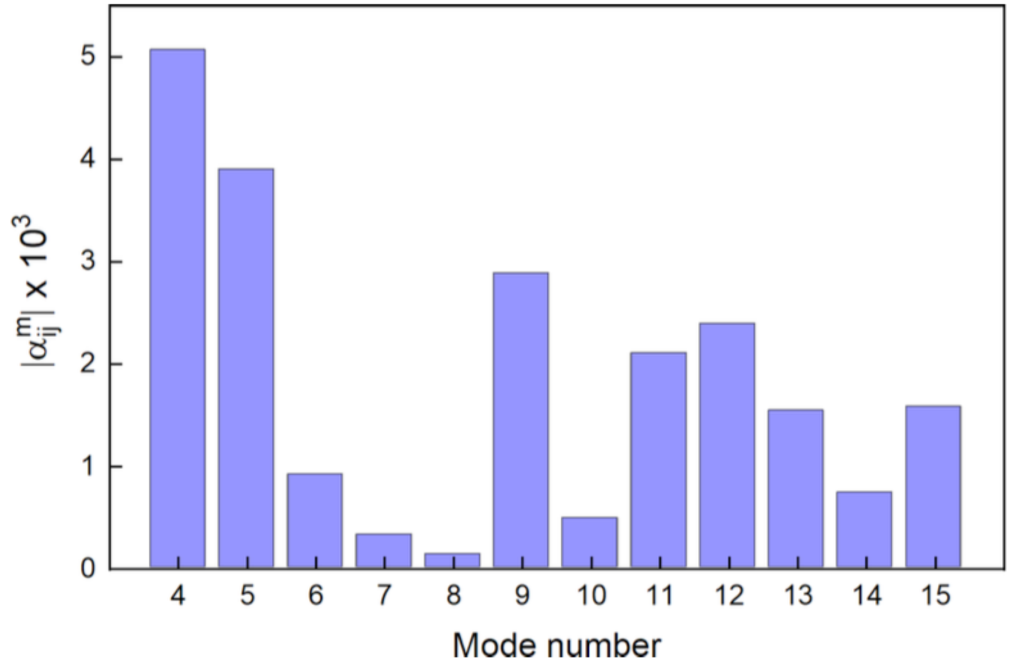


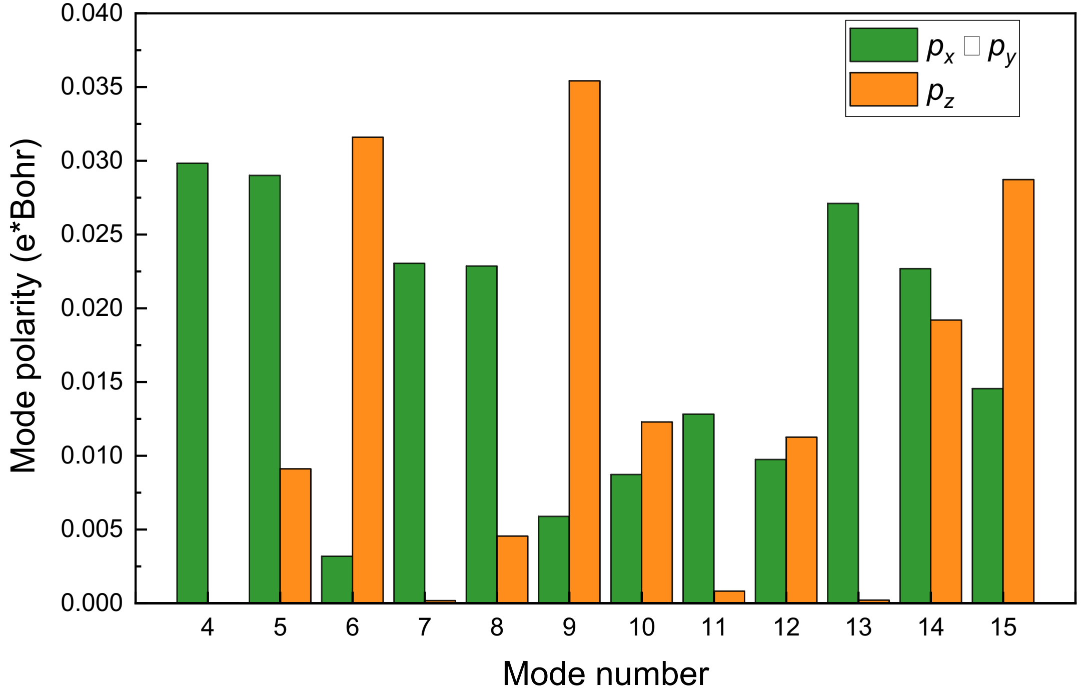


- The lowest frequency mode shows the strongest Raman response.
- Combined with the mode polarity, mode 4 contributes to Pockels tensor significantly.

# Ionic Pockels tensor for *Cm* $BaTiO_3$

$$4\pi \sum_m \frac{1}{\omega_m^2} \left( \sum_{\kappa,\alpha} \frac{\partial \chi_{ij}^{(1)}(\mathbf{R}, \eta_0)}{\partial \tau_{\kappa\alpha}} u_m(\kappa\alpha) \right) \times \left( \sum_{\kappa',\beta} Z^*_{\kappa',\gamma\beta} u_m(\kappa'\beta) \right)$$

| [111] | $[1\bar{1}1]$ | $[\bar{1}11]$ | $[\bar{1}\bar{1}1]$ |
|---|---|---|---|
| $\begin{bmatrix} 1812 & -1583 & -25 \\ -1584 & 1812 & -25 \\ -11 & -11 & 41 \\ -767 & 824 & -6 \\ 817 & -760 & -6 \\ 22 & 52 & -12 \end{bmatrix}$ | $\begin{bmatrix} 1811 & 1582 & -25 \\ -1583 & -1810 & -25 \\ -11 & 11 & 41 \\ 767 & 824 & 6 \\ 817 & 759 & -6 \\ -22 & 52 & 12 \end{bmatrix}$ | $\begin{bmatrix} -1806 & -1578 & -25 \\ 1578 & 1806 & -25 \\ 11 & -11 & 41 \\ 765 & 822 & -6 \\ 815 & 757 & 6 \\ 22 & -52 & 12 \end{bmatrix}$ | $\begin{bmatrix} -1810 & 1581 & -25 \\ 1582 & -1809 & -25 \\ 11 & 11 & 41 \\ -766 & 823 & 6 \\ 816 & -758 & 6 \\ -22 & -52 & -12 \end{bmatrix}$ |

| Electronic Pockels Tensor (pm/V) | Ionic Pockels Tensor (pm/V) |
|---|---|
| $\begin{bmatrix} 0 & 0 & 0.7 \\ 0 & 0 & 0.7 \\ 0 & 0 & 2 \\ 0 & 0.76 & 0 \\ 0.76 & 0 & 0 \\ 0 & 0 & 0 \end{bmatrix}$ | $\begin{bmatrix} 1.8 & 0.5 & -25 \\ -1.8 & 0.25 & -25 \\ 0 & 0 & 41 \\ 0.25 & \boxed{823} & 0 \\ 816 & 0.5 & 0 \\ 0 & 0 & 0 \end{bmatrix}$ |

Exp. $r_{42}^{\text{clamped}} = 730$ pm/V



Zgonik *et al.*, Phys. Rev. B 50, 5941 (1994)

# Difference between Raman active and inactive mode

$$\left(\sum_{\kappa,\alpha}\frac{\partial\chi^{(1)}_{ij}(\mathbf{R},\eta_0)}{\partial\tau_{\kappa\alpha}}u_m(\kappa\alpha)\right)$$

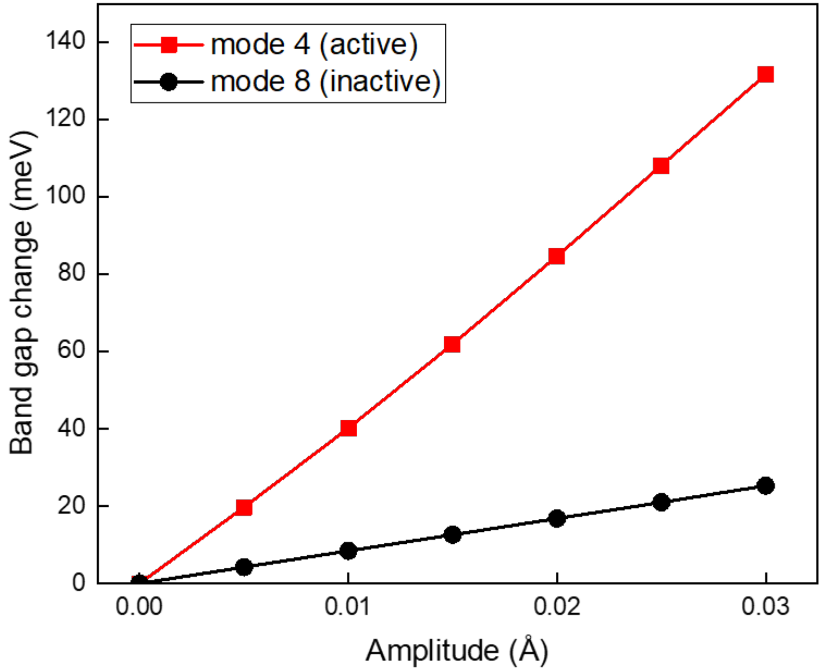


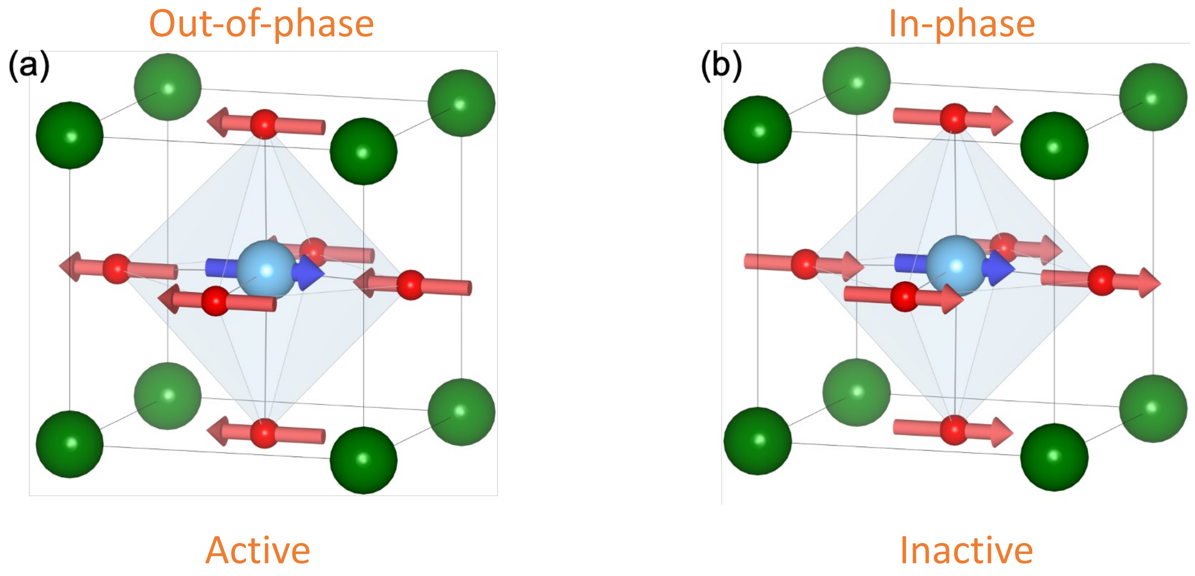


- Active mode changes the orbital overlap and bond length significantly.
- Inactive mode shows the translation characteristic.

# Piezo Electro-Optic tensor

Piezoelectric tensor

$$r^{piezo}_{ij\gamma} = \underline{p_{ij\mu\nu}}\,\overline{d_{\gamma\mu\nu}}$$

Elasto-optic tensor

$$p_{ij\mu\nu} \approx \frac{\Delta(\varepsilon^{-1}_{ij})(\eta^{+}) - \Delta(\varepsilon^{-1}_{ij})(\eta^{-})}{2\eta_{\mu\nu}} + \mathcal{O}(\eta^2)$$ Finite difference method

| Elasto-optic Element | *Cm* | *P4mm* | Expt. [67] |
|---|---|---|---|
| $p_{11}$ | 0.93 | 0.53 | 0.50 |
| $p_{12}$ | 0.058 | 0.61 | 0.11 |
| $p_{13}$ | 0.087 | 0.42 | 0.2 |
| $p_{31}$ | 0.037 | 0.37 | 0.07 |
| $p_{33}$ | 0.80 | 0.0085 | 0.77 |
| $p_{44}$ | 0.81 | 0.17 | 1.0 |

Main contribution for $r_{42}$

| | This work | Other Theory [68] | Expt. |
|---|---|---|---|
| $d_{31}$(pC/N) | 40 | 15 | 33 [67], 34 [69] |
| $d_{33}$(pC/N) | 38 | 90 | 90 [67], 85.6 [69] |
| $d_{42}$(pC/N) | 469 | 10 | 282 [67], 392 [69] |

Main contribution for $r_{42}$

| Elasto-optic Element | *Cm* | *P4mm* | Expt. [67] |
|---|---|---|---|
| $r^{\text{piezo}}_{13}$(pm/V) | 3.5 | 2 | −2 |
| $r^{\text{piezo}}_{33}$(pm/V) | 30 | 6 | 65 |
| $r^{\text{piezo}}_{42}$(pm/V) | 760 | 81 | 570 |

*Cm* phase gives the better result

- *Cm* phase provides a better explanation of piezo EO tensor compared to *P4mm* phase



Detraux and Gonze , Phys. Rev. B. 63, 115118 (2001)
Bellaiche *et al.*, Phys. Rev. Lett. 115, 267602 (2015)

PHYSICAL REVIEW B **108**, 115201 (2023)

# Nature of electro-optic response in tetragonal $BaTiO_3$

Inhwan Kim, Therese Paoletta, and Alexander A. Demkov*
*Department of Physics, The University of Texas, Austin, Texas 78712, USA*

(Received 15 June 2023; revised 7 August 2023; accepted 29 August 2023; published 11 September 2023)

Barium titanate, $BaTiO_3$ (BTO), has emerged as a promising electro-optic material with applications in silicon photonics. It boasts one of the largest known electro-optic coefficients; however, the origin of this giant electro-optic response has not been investigated in detail and is poorly understood. Here we report on a first-principles study of the electro-optic or Pockels tensor in tetragonal *P4mm* BTO. We find good agreement with experiment if the *P4mm* structure is viewed as a dynamic average of four lower symmetry *Cm* structures. The large value of the Raman component of the EO coefficient is attributed to a low frequency and strong electron-phonon coupling of the lowest optical mode, and we trace the equally large piezoelectric contribution to the large components of the piezoelectric and elasto-optic tensors.

DOI: 10.1103/PhysRevB.108.115201

# Conclusions

$$\boxed{r_{ij\gamma}^{elec} + r_{ij\gamma}^{ion} + r_{ij\gamma}^{piezo}}$$

[111]-averaged tetragonal phase

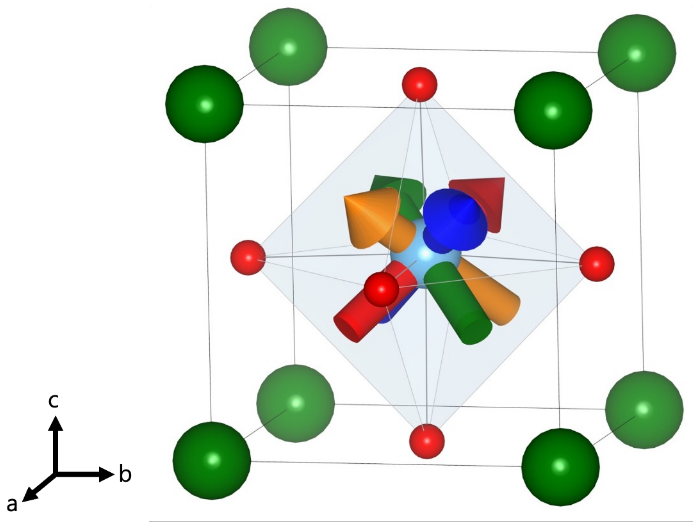


| Theory: Unclamped Pockels tensor ($^{pm}/_{V}$) | Experiment: Unclamped Pockels tensor ($^{pm}/_{V}$) |
|---|---|
| $\begin{bmatrix} 0 & 0 & 21.5 \\ 0 & 0 & 21.5 \\ 0 & 0 & 70 \\ 0 & 1560 & 0 \\ 1560 & 0 & 0 \\ 0 & 0 & 0 \end{bmatrix}$ | $\begin{bmatrix} 0 & 0 & 8 \\ 0 & 0 & 8 \\ 0 & 0 & 105 \\ 0 & 1290 & 0 \\ 1290 & 0 & 0 \\ 0 & 0 & 0 \end{bmatrix}$ |

- **Piezoelectric electro-optic response contributes almost a half of the Pockels tensor**
- **Cm averaged tetragonal phase better explains the linear electro-optic response than *P4mm***
- **Strong EO response comes from the combination of a low phonon frequency and Raman-active mode.**



Zgonik *et al.*, Phys. Rev. B 50, 5941 (1994)

# Future work

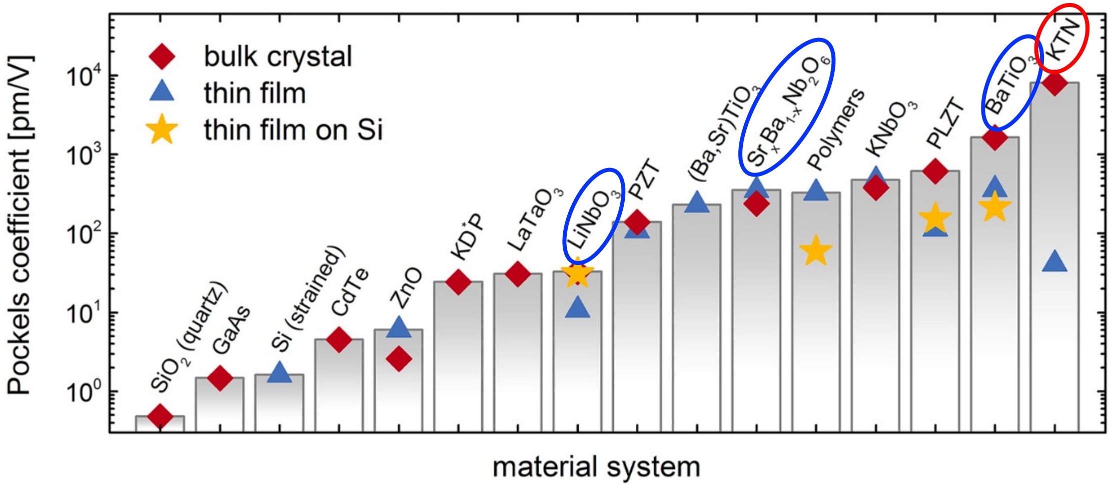


- **Identifying microscopic origin in $LiNbO_3$**
- **Calculating Pockels response in $KTa_{0.5}Nb_{0.5}O_3$**
- **Calculating ionic and piezo Pockels response in VASP using finite difference**
- **Exploring the how the domain structure affect the Pockels response**

# Supplementary materials

# The Linear Electro-Optic Response: the Pockels Effect

$$\Delta\left(\frac{1}{n^2}\right) = \Delta\left(\varepsilon^{-1}\right)_{ij} = \sum_{\gamma} r_{ij\gamma} E_{\gamma}$$

$r_{ij\gamma}$: Pockels coefficient (tensor) or electro-optic tensor

$$\Delta\left(\varepsilon^{-1}\right)_{ij} = -\varepsilon_{im}^{(-1)} \Delta\varepsilon_{mn} \varepsilon_{nj}^{(-1)}$$

$R$: coordinate, $\eta$: strain, $E$: electric field

$$\left[\frac{d\varepsilon_{ij}(\mathbf{R},\eta_0,E)}{dE_{\gamma}}\right]_{\mathbf{R}_0,\eta_0,E=0} = \left[\frac{\partial\varepsilon_{ij}(\mathbf{R},\eta_0,E)}{\partial E_{\gamma}}\right]_{E=0} + \underbrace{\left[\frac{\partial\varepsilon_{ij}(\mathbf{R},\eta_0,E)}{\partial \tau_{\kappa\alpha}}\right]_{\mathbf{R}_0} \boxed{\frac{\partial \tau_{\kappa\alpha}}{\partial E_{\gamma}}}}_{\text{Ionic term}} + \underbrace{\left[\frac{\partial\varepsilon_{ij}(\mathbf{R},\eta_0,E)}{\partial \eta_{\mu\nu}}\right]_{\eta_0} \frac{\partial \eta_{\mu\nu}}{\partial E_{\gamma}}}_{\text{Piezoelectric term}}$$

Expand the full differential of the dielectric tensor into electronic, ionic, and piezoelectric contributions

# Clamped Electro-Optic Response

| Electronic Pockels tensor ($^{pm}/_{V}$) | Ionic Pockels tensor ($^{pm}/_{V}$) |
|---|---|
| $\begin{bmatrix} 0 & 0 & 0.7 \\ 0 & 0 & 0.7 \\ 0 & 0 & 2 \\ 0 & 0.76 & 0 \\ 0.76 & 0 & 0 \\ 0 & 0 & 0 \end{bmatrix}$ | $\begin{bmatrix} 0 & 0 & -25 \\ 0 & 0 & -25 \\ 0 & 0 & 40 \\ 0 & 820 & 0 \\ 820 & 0 & 0 \\ 0 & 0 & 0 \end{bmatrix}$ |

| Clamped Pockels tensor (exp.) ($^{pm}/_{V}$) |
|---|
| $\begin{bmatrix} 0 & 0 & 10 \\ 0 & 0 & 10 \\ 0 & 0 & 40 \\ 0 & 720 & 0 \\ 720 & 0 & 0 \\ 0 & 0 & 0 \end{bmatrix}$ |

- *Cm* phase provides a better explanation of piezo EO tensor compared to *P4mm* phase

Zgonik *et al.*, Phys. Rev. B 50, 5941 (1994)

# Elasto-Optic Tensor Test Calculations

$$\underline{r_{ij\gamma}^{piezo}} \quad = \quad p_{ij\mu\nu} d_{\gamma\mu\nu} \qquad\qquad p_{ij\mu\nu} \approx \frac{\Delta(\varepsilon_{ij}^{-1})(\eta^{+}) - \Delta(\varepsilon_{ij}^{-1})(\eta^{-})}{2\eta_{\mu\nu}} + \mathcal{O}(\eta^2)$$

| | LDA | PBE | PBEsol | LDA (QE) | Other theory references | Experiment |
|---|---|---|---|---|---|---|
| Si | | | | | | |
| $p_{11}$ | −0.0914 | −0.105 | −0.0971 | −0.101 | −0.098, −0.111 | −0.094 |
| $p_{12}$ | 0.0124 | 0.0121 | 0.0152 | 0.010 | 0.007, 0.020 | 0.017 |
| Diamond | | | | | | |
| $p_{11}$ | −0.261 | −0.268 | −0.262 | −0.263 | −0.264 | −0.248 |
| $p_{12}$ | 0.0734 | 0.0471 | 0.0717 | 0.061 | 0.076 | 0.044 |
| NaCl | | | | | | |
| $p_{11}$ | 0.0727 | 0.101 | 0.0943 | 0.058 | 0.077 | 0.155 |
| $p_{12}$ | 0.16 | 0.163 | 0.171 | 0.153 | 0.157 | 0.161 |
| MgO | | | | | | |
| $p_{11}$ | −0.3 | −0.292 | −0.2859 | −0.299 | −0.310, −0.218 | −0.259 |
| $p_{12}$ | −0.42 | −0.0545 | −0.04627 | −0.042 | −0.050, 0.013 | −0.011 |

- Finite difference to calculate the elasto-optic tensor (Voigt notation)
- The test calculation describes the elasto-optic tensor fairly well compared to corresponding experiment value